RESEARCH ARTICLE

Elizabeth McClelland · Colin J. N. Wilson ·
Leon Bardot

Palaeotemperature determinations for the 1.8-ka Taupo ignimbrite, New Zealand, and implications for the emplacement history of a high-velocity pyroclastic flow

Abstract Palaeomagnetic data from lithic clasts collected at 46 sites within layers 1 and 2 of the 1.8-ka Taupo ignimbrite, New Zealand, have been used to determine the palaeotemperatures and thermal structure of the deposit on its emplacement. Equilibrium temperatures from sites less than 30–40 km from vent are 150–300 °C, whereas at greater distances site equilibrium temperatures increase up to 400–500 °C. This variation is seen in both layer 1 and 2 deposits, with values for layer 1 being somewhat cooler, and with its increase in temperature occurring at a greater distance from vent. A temperature maximum at ~50 km from vent coincides with a zone of pink thermal-oxidation colouration of pumices previously inferred to reflect higher emplacement temperatures. Additional palaeomagnetic data collected by us and others from pumice clasts show comparable temperature variations, but these temperature estimates are shown here to be due to a chemical remanence and unreliable for accurate temperature estimates. Cooler temperatures in proximal parts of the ignimbrite are consistent with admixture of >20% cold lithic clasts at source and interaction with the pre-eruption Lake Taupo. The similar, but offset, increases in equilibrium temperatures for medial and distal layers 1 and 2 are consistent with both layers being deposited from the same flow. However, any proximal deposits left by the later, hotter material must have been subsequently eroded, or be so thin that our collection failed to sample them. Radial asymmetries in equilibrium temperatures as well as other physical parameters suggest that the deposit emplacement temperature is primarily determined at source, rather than by interaction with air during transport. These data support

previous interpretations that a concentrated basal flow played a dominant role in emplacement and deposition of the Taupo ignimbrite.

Introduction

A key piece of information in understanding the dynamics of explosive eruptions is given by the temperatures at which pyroclastic deposits are emplaced. If the original magmatic temperature can be estimated (e.g. from Fe–Ti oxide compositions; Lindsley 1991), and contributions to cooling from such effects as adiabatic decompression and the incorporation of cold country-rock fragments quantified, emplacement temperatures provide constraints on the degree of interaction between the erupting pyroclastic mixture and the atmosphere or external water. A major challenge is in applying these ideas towards interpreting the emplacement histories of ignimbrites, which are the most-voluminous pyroclastic deposits known. Ignimbrites show evidence for a wide range of emplacement temperatures, from intensely welded deposits which may be confused with lava flows and probably have cooled by <50 °C from magmatic temperatures (e.g. Henry and Wolff 1992), to non-welded deposits which show textural evidence for liquid water being present in their matrices during emplacement, indicating temperatures of <100 °C (e.g. Minoan phase 3; Sparks and Wilson 1990).

A general subdivision is made of ignimbrites into two main classes, welded and non-welded, the onset of welding at any point in an ignimbrite being primarily determined by the juvenile composition (including retained volatiles which would lower glass viscosities), load stresses, and temperature (both the absolute value and the time spent above any given value, i.e. the cooling rate). Typical temperatures for the onset of welding are estimated or measured at between 500 and 650 °C for calc-alkaline

E. McClelland · L. Bardot
Department of Earth Sciences,
University of Oxford,
Parks Road, Oxford, OX1 3PR, UK

C. J. N. Wilson (✉)
Institute of Geological & Nuclear Sciences,
PO Box 30368, Lower Hutt 6315, New Zealand
e-mail: C.Wilson@gns.cri.nz

compositions (Friedman et al. 1963; Yagi 1966; Riehle 1973; Bierwirth 1982 (cited in Cas and Wright 1987); Riehle et al. 1995), but most welded ignimbrites, regardless of emplacement temperature, include some material which is non-welded due to either rapid cooling (e.g. directly overlying a cold substrate) or inadequate load stresses (e.g. the topmost part of the deposit).

In welded ignimbrites, the emplacement temperature can in principle be determined from the maximum intensity of welding (as reflected in bulk densities) coupled with estimates of the load stress (Kono and Osima 1971; Riehle 1973; Riehle et al. 1995; although see Wilson and Hildreth 2003). However, non-welded deposits require alternative approaches. A number of techniques have been used, including infrared spectroscopy of carbonised wood fragments (Maury 1971), observations of oxidation colours in pumice clasts (Tsuboi and Tsuya 1930), palaeo-magnetism of the deposits themselves (Aramaki and Akimoto 1957), and palaeomagnetism of individual clasts within the deposits (Hoblitt and Kellogg 1979).

Of the methods listed above, palaeomagnetic determinations on country-rock lithic clasts incorporated into ignimbrites represent a powerful tool which can quantitatively determine emplacement temperatures from ~150 °C up to the highest-temperature Curie point (T_c) of the Fe–Ti oxide species in the deposit (typically magnetite, T_c= 580 °C; Bardot and McClelland 2000). Such palaeomagnetic techniques are thus applicable in non-welded ignimbrites to temperatures which can, in principle, complement those which can be estimated from welding intensities in higher-temperature deposits. Palaeomagnetic techniques have been applied to a number of non-welded ignimbrites (and other pyroclastic deposits) from Vesuvius (Kent et al. 1981), Santorini (McClelland and Druitt 1989; McClelland and Thomas 1990; Bardot et al. 1996; Bardot 2000), and Krakatau (Mandeville et al. 1994). However, such studies have concentrated on limited portions of deposits, and there has not been a systematic study of a well-exposed ignimbrite. Here we present the results of a regional study of palaeotemperature estimates from lithic-clast palaeomagnetism for the widespread, non-welded 1.8-ka Taupo ignimbrite in New Zealand.

The Taupo ignimbrite was used as a test case for this work for several reasons.

1. Its youth, lack of weathering and totally non-welded nature, with no devitrification or significant vapour-phase alteration, apart from thermal-oxidation colours in some areas.
2. Its thin, widespread nature which allowed sampling through much or all of its thickness.
3. The ignimbrite incorporates a significant amount of mostly fresh lithic clasts (2.1 km^3 in total; Wilson 1985), most lithologies of which are well suited to palaeomagnetic studies. In this study, rock clasts used are almost entirely igneous lithologies which can be inferred to have been derived from the vent area (e.g. Cole et al. 1998), and not been picked up from the ground surface during transport.
4. The ignimbrite is rich in carbonised vegetation fragments, from leaves to 1-m-diameter logs, the carbonisation state of which provides an independent semi-quantitative (for the purposes of this study) indicator of temperature.
5. The physical volcanology of the ignimbrite has been documented in considerable detail to the extent that it is an archetypal representative of the deposits termed low-aspect ratio ignimbrites, that is, having a low ratio of average thickness to the diameter of a circle of equal area to the deposit (Walker et al. 1980).

Reconstructions of the emplacement dynamics using deposit characteristics imply the ignimbrite was deposited from a short-lived pyroclastic density current travelling at speeds of the order 200–300 m/s (Wilson and Walker 1981). However, the nature of the current is disputed. Wilson (1985, and references therein) interpreted the bulk of the current to be a concentrated flow (solids volume fractions of the order of tens of percent), based on the distribution of coarse, light pumice clasts and light, fine-grained fractions in the deposit, and on the presence of a distinctive and characteristic suite of depositional facies (see below). In contrast, Dade and Huppert (1996) presented a model for the flow as a dilute (solids volume fractions of 0.3%), homogeneous density current, based on a fitting of theoretical predictions from the model versus gross lateral variations in one of the facies in the ignimbrite (see Wilson (1997) and Dade and Huppert (1997) for further debate). Part of the motivation for the present study is the notion that if the palaeotemperature of any part of the flow could be calculated, then the degree of atmospheric interaction (and hence dilution of the current) may be better assessed.

A previous palaeomagnetic study, on pumice clasts from the Taupo ignimbrite by Bahar et al. (1993), reported a difference in magnetic behaviour, and hence cooling histories, between pumice clasts from 'proximal' (5–34 km from vent) versus 'distal' (36–46 km) localities. The authors inferred minimum temperatures of 220–300 °C at 'proximal' sites and higher values of 450–585 °C at the 'distal' sites. Cooling was inferred to have been slower at distal sites, and was linked by Bahar et al. (1993) to observations by Wilson (1985) of a lower content of country-rock lithic clasts, higher content of <1 mm ash and development of thermal-oxidation colouration in areas farther from vent. However, emplacement temperature estimates from pumices have been demonstrated elsewhere to be incorrect because of post-emplacement alteration of the magnetic minerals (McClelland and Druitt 1989; Donoghue et al. 1999). Our results presented here broadly agree with those of Bahar et al. (1993) but we infer this agreement to be spurious because, as we show, variations in maximum unblocking temperature in pumices are a function of a change in mineralogy with distance from source.

Table 1 Summary of the deposits and activity during the Taupo eruption

Phase or unit	Name of deposit	Type of deposit	Interaction with Lake Taupo?	Notes
1	Initial ash	Fall	Yes	Minor activity at start of eruption
2	Hatepe plinian pumice	Fall	No	Dry, powerful fall activity
3	Hatepe ash	Fall	Yes	Wet-deposited, pumice-rich, hence pale grey colour Followed by erosion break
4	Rotongaio ash	Fall	Yes	Wet-deposited, obsidian-rich, hence dark grey colour
5 *and*	Taupo plinian pumice *and*	Fall *plus*	No	Dry, powerful fall activity *accompanied by*
6	Early ignimbrite flow units	Ignimbrite	(displaced lake)	Localised flow activity
7	Taupo ignimbrite	Ignimbrite	Yes	Devastating, widespread flow deposit

Taupo ignimbrite

The Taupo ignimbrite formed during the climactic phase of the 1.8-ka Taupo eruption (cf. Table 1), over a period of ~400 s (Wilson and Walker 1981), from a source centred on the Horomatangi Reefs area of Lake Taupo (Fig. 1). Country-rock fragments in the Taupo ignimbrite are dominated by fresh rhyolite lava (mostly devitrified, less often glassy or vapour-phase altered), with minor welded ignimbrite, andesite lava, greywacke and indurated lacustrine sediments (Chernet 1987; Cole et al. 1998). Limited petrographic and analytical data imply that many of the rhyolite lithics were derived from domes extruded during post-12 ka eruptions at Taupo (Chernet 1987; Sutton et al. 1995; Cole et al. 1998; Sutton et al. 2000). This, coupled with information on the vent positions inferred from the post-12 ka fall deposits and possible coeval dome extrusions (Wilson 1993), and with current understanding of evolving vent positions during the Taupo eruption (Smith and Houghton 1995), is used to infer that the Taupo ignimbrite vent probably intersected a subaerial, elongate cluster of domes. These domes were probably connected by dry land to the eastern side of the lake, but surrounded by water ~100 m or more deep around a >180° arc from northeast through west to the southwest. In the context of this study, it is important to note that in most areas where the Taupo ignimbrite was sampled, there are no exposed surficial rock types which match the lithic fragments sampled in the ignimbrite. Thus, it can be assumed that the lithics sampled for this work represent material incorporated at the source.

The Taupo ignimbrite covers a near-circular area extending to a distance of 80±10 km from vent (Fig. 1), has a bulk volume of ~30 km^3 (equivalent to ~10 km^3 magma plus 2.1 km^3 lithics), and hence an average thickness of only ~1.5 m (Wilson 1985). This thin, widespread nature of the ignimbrite is interpreted to reflect the exceptionally high velocity of the parental flow (Walker et al. 1980). There are two striking features of the deposit (Fig. 2) which also reflect the energetic nature of the parental density current.

The first feature is that, like many other ignimbrites (Sparks et al. 1973; Sparks 1976), the Taupo consists of two layers, 1 and 2 (the fall-derived layer 3 of Sparks et
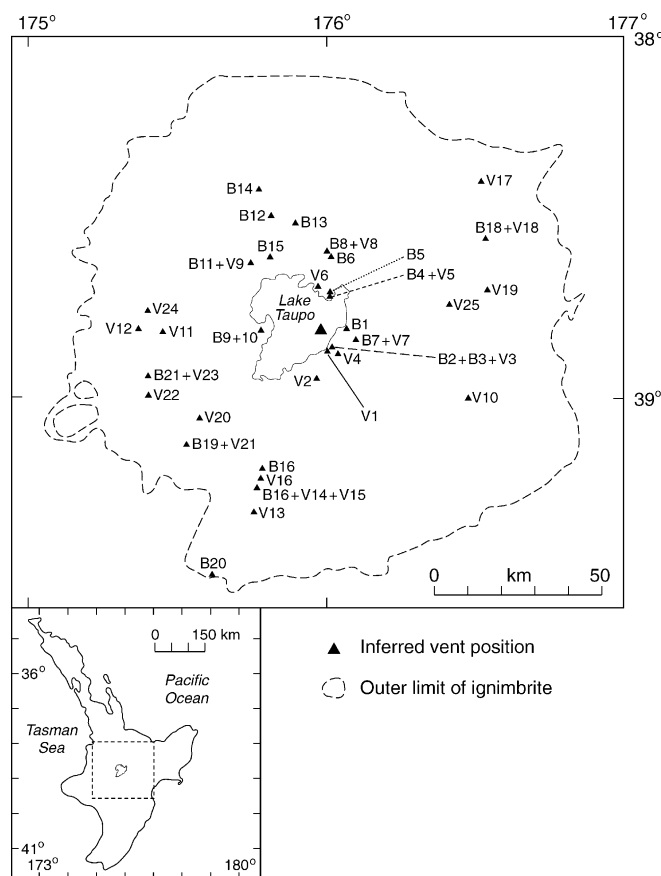

Fig. 1 Map showing the area covered by the Taupo ignimbrite (after Wilson 1985) and the sites sampled in this study. (TP)*B* refers to layer 1 sites and (TP)*V* to layer 2 sites

al. (1973) is rarely preserved at Taupo and not discussed further). Layer 1 represents portions of the ignimbrite affected by processes inferred to have occurred at the flow front in response to interaction with the ground surface (including vegetation) and the atmosphere (Wilson and Walker 1982). At Taupo, layer 1 is generally thinner than layer 2, and contains a greater abundance of lithic clasts, which are also larger (Wilson 1985). There are two facies in layer 1, a lower, thicker one which is dominated by pumice and has variable contents of fine
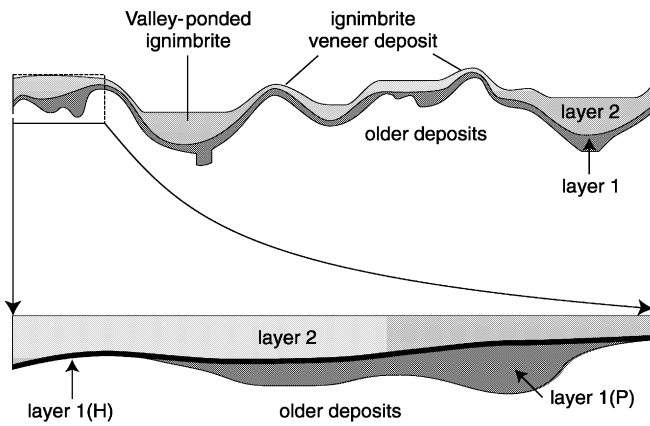
Fig. 2 Schematic diagram to illustrate the stratigraphic relationships between layers 1 and 2 of the Taupo ignimbrite, and the morphological relationships between the ignimbrite and the underlying landscape surface. Layer 1P is typically 20 cm to 6 m thick, and is thicker in depressions. Layer 1H is thinner (rarely >1 m) but more uniform in thickness, and is richer in lithics. The two layer 2 facies are of very similar physical composition but show strong morphological relationships to the underlying landscape. See Walker et al. (1980; 1981a, 1981b) and Wilson (1985) for more details

ash matrix (layer 1P), and an upper, thinner one which is rich in dense (lithic and crystal) components and lacks a fine ash matrix (layer 1H). Layer 1P is inferred to represent material which was jetted off the front of the moving current by the explosive expansion of ingested air, and which variably interacted with abundant vegetation (Wilson and Walker 1982). Layer 1H is inferred to represent coarse/dense material which was segregated by gas streaming through the frontal parts of the current, sedimented to the base of the current, and sheared out to form a thin ground layer (Walker et al. 1981a).

Layer 2 represents most of the Taupo deposit, and is inferred to be material left behind from the body and tail of the current as it spread over the landscape. It consists of two facies, landscape-mantling veneer deposits, and landscape-modifying valley-ponded ignimbrite. These two facies have contrasting geometries (see below) but similar grain-size and component characteristics, the only difference being that coarse pumice clasts are preferentially found in the valley-ponded ignimbrite (Walker et al. 1981b).

The second striking feature is that the ignimbrite has two contrasting morphological expressions, largely reflecting, and defined by, the difference between the veneer and valley-ponded facies of layer 2 (Fig. 2). Roughly 90% of the area but somewhat less than 50% of the volume of ignimbrite is represented by landscape-mantling deposits, which cover the pre-eruption palaeotopography with material ranging in thickness from ~10 m in proximal areas to 15–30 cm in distal areas. The remainder of the deposit is represented by landscape-modifying material, which ponded in valley bottoms and low-lying areas to thicknesses of up to 70 m. The thickness of the ponded

materials does not vary systematically with distance from source. Most of the thickness variations are seen in layer 2; layer 1 (particularly layer 1P) does thicken somewhat into depressions, but to a much lesser extent.

A general model for the Taupo current (Wilson 1985) envisages it travelling at high velocities over most of the landscape within 80 km of vent, generating layer 1 deposits at the front of (jetted deposits) and beneath (ground layer) the moving flow, and leaving behind part of the body of the current which was slowed by ground friction. As the material left behind slowed, it became increasingly affected by the local topographic relief, and some fraction drained into low-lying areas to form the valley-ponded ignimbrite, leaving behind remnants as veneer deposit. Thus, the thickness and volume of individual valley ponds primarily reflect the amount of material which drained off the valley walls, and hence the size and steepness of the valley catchment, rather than any preferential passage of the current along valley floors.

Existing data and models for the Taupo ignimbrite (Wilson 1985, and references therein) include the following, which are relevant to interpreting the palaeomagnetic results below. First, the ignimbrite was erupted and emplaced in one short-lived episode, with no evidence for any time breaks long enough to permit cooling between different batches of material. Second, the different depositional facies in layers 1 and 2, seen at any given distance from vent, were derived from a single current, not successive currents of contrasting properties. Thus, for example, the lithic-richer layer 1H deposits were derived from material which also deposited (somewhat farther from vent) layer 2, and hence lithic clasts in these different facies will share, to a first order, a common history in the parental current. Third, lithic fragments in the material which erupted earliest were more numerous and larger than those in the bulk of the deposit. Fourth, the content of lithic fragments relative to crystals varies spatially, with deposits to the northeast and southwest having higher and lower proportions of lithics respectively (Wilson 1985, Fig. 67). Regional asymmetries are also shown by the distribution of thermal-oxidation colours in the pumices and matrix of layer 2 (Wilson 1985, Fig. 28).

Palaeotemperature techniques

Review of existing methodologies and techniques

Aramaki and Akimoto (1957) were the first to use magnetism to infer palaeotemperatures. They used natural remanent magnetization (NRM), which is a vector sum of the component magnetizations, in a qualitative manner to distinguish between hot pyroclastic flows and cold mudflows. They assumed that if a deposit was emplaced hot (i.e. at $T>T_c$ for the constituent magnetic minerals), then the NRMs of fragments contained within the deposit would all be parallel to the Earth's field direction acquired during cooling whereas, if a deposit was emplaced cold, then the NRMs of the fragments would be randomly

oriented by flow processes. This method was extended by Hoblitt and Kellogg (1979), using progressive thermal demagnetization to give specific emplacement temperature (T_{emp}) estimates for lithics incorporated into the deposits. Most subsequent work has also used progressive thermal demagnetization of non-juvenile material (e.g. Kent et al. 1981; McClelland and Druitt 1989; Bardot 2000).

Emplacement temperature determination

Pyroclastic eruptions involve the transfer of fragmented magma (together with phenocrysts, dissolved volatiles, and country-rock lithic material entrained from the conduit walls) from some depth onto the Earth's surface. In pyroclastic density currents, lithic fragments may also be picked up from the ground surface during transport, but the lithologies sampled in the Taupo ignimbrite are all demonstrably vent-derived. Lithic clasts derived from the conduit walls will have been magnetized prior to the eruption. If the pyroclastic deposits were emplaced at temperatures above those of the places from where the lithics were derived, then the lithic clasts will have been heated during their incorporation into the current and deposit, and then cooled to ambient temperature in their present position. On incorporation, a portion of the original magnetization, with blocking temperatures (T_b) less than or equal to the maximum temperature of the deposit, will have been demagnetized and replaced by a new partial thermoremanence (pTRM) on subsequent cooling. The original high-T_b remanence within each clast will have a random orientation, whereas the new low-T_b remanence will have the same orientation in each clast, parallel to the local Earth's magnetic field at the time of cooling.

The value of T_{emp} of a lithic clast can thus be determined by progressive thermal demagnetization. The lithic sample is heated and cooled in a magnetic field of less than 5 nT and the remanence is measured. The heating and cooling is repeated at increasing peak temperatures, measuring remanence after each application of a temperature step. This process demagnetizes the grains with T_b values less than or equal to the peak temperature reached in the respective heating cycle, and an increment of the total remanence is removed at each step. At temperatures up to the T_{emp}, the low-T_b (Earth's field) component will be removed; above T_{emp} the original high-T_b component is removed. The estimate of T_{emp} is thus in the interval between the highest temperature at which the low-T_b Earth's field magnetization is still present and the next highest temperature where it is lost.

Some authors have cited estimates of emplacement temperatures from juvenile material (e.g. Downey and Tarling 1984; Bahar et al. 1993). Juvenile pumice clasts only have a single component of magnetization, parallel to the ambient Earth's magnetic field at the time of the eruption, because they have no magnetic history prior to the eruption. These authors derived an emplacement temperature from the maximum unblocking temperature of this Earth's field component. This technique would indeed give a valid emplacement temperature estimate, provided that the magnetic mineralogy of the juvenile component remained unchanged after deposition. For example, consider a pumice clast containing magnetite grains with T_c=580 °C, which had cooled during transport to its emplacement in ignimbrite with a temperature of 400 °C. Magnetic grains with blocking temperatures above T_{emp} would have blocked-in a remanence while the clast was tumbling randomly in the flow, and the resultant sum of all remanence fractions acquired above T_{emp} would average to zero. Once the clast came to rest, a partial TRM would be acquired in the grains with lower blocking temperatures. Thermal demagnetization of the remanence of this clast would show that all remanence would be removed by heating to 400 °C in the laboratory. The reliability of the emplacement temperature estimated in such an example can be tested by monitoring the variation of magnetic susceptibility with temperature to determine the T_c value of the magnetic-mineral assemblage. The susceptibility should remain high until the T_c of 580 °C is reached, regardless of the fact that the remanence would decay to zero at 400 °C. However, such a high susceptibility has not been observed in any pyroclastic deposits studied by us. All juvenile vesicular material appears to carry a single-component remanence in all blocking temperature intervals right up to $T=T_c$, regardless of the emplacement temperature of the deposit (Zlotniki et al. 1984; McClelland and Druitt 1989; Donoghue et al. 1999). Our preferred explanation for this is that post-emplacement resorbtion of volatiles causes a significant alteration of the magnetic mineralogy, which thus acquires a chemical remanent magnetism (CRM), not a TRM. This, however, has not been rigorously tested. Blocking temperatures of CRM will extend up to the T_c of the mineral phase, irrespective of the reaction temperature (McClelland 1996).

Cooling-rate correction

The temperature at which the magnetization of a given grain is unblocked is dependent on the timescale of the heating process (Dodson and McClelland-Brown 1980), such that under conditions of cooling in a deposit, a particular magnetic grain will block over a longer timescale at a lower temperatures. Therefore, a cooling-rate correction should, in principle, be applied when temperatures are estimated from laboratory unblocking temperatures (T_{ub}). Laboratory-based measurements will be overestimates, as the laboratory timescales usually will be shorter than those of the natural cooling. Natural cooling rates can be estimated from heat conduction calculations (e.g. Jaeger 1964). For a 1.5-m-thick sheet (e.g. the Taupo veneer deposit), cooling to 50% of initial temperature in the centre of the deposit would occur in ~15 h, which equates to a cooling rate of 10^{-2} °C/s. For a 20-m-thick sheet (a typical thickness for the valley-pond ignimbrite),

the centre of the deposit would have cooled to 50% of initial temperature in 4 months (neglecting the additional, second-order cooling due to infiltration of rain or groundwater), which equates to a cooling rate of 0.5×10^{-4} °C/s. Dodson and McClelland-Brown (1980) presented graphs of natural blocking temperatures against laboratory unblocking temperatures for various natural cooling rates. Natural blocking and laboratory unblocking temperatures are virtually equivalent for a cooling rate of 10^{-2} °C/s, so there is no need to apply a correction for the Taupo veneer deposit or ground layer. A cooling-rate correction does need to be applied for the valley-pond sites, as a cooling rate of 0.5×10^{-4} °C/s results in laboratory demagnetization at 250 °C of a remanence blocked at 200 °C in nature, i.e. the cooling-rate correction is −50 °C. The magnitude of the correction reduces at higher temperatures and is −30 °C for laboratory unblocking at 450 °C, and −10 °C for laboratory unblocking at 515 °C.

Temperature validation (general principles)

The palaeomagnetic technique may give erroneous results if the magnetic mineralogy of a lithic clast has altered during the eruption. This could give a CRM overprint which may partly or completely replace the primary remanence in T_b intervals which extend above the T_{emp}. This is because T_b values of a CRM are controlled by the grain size of the new or modified magnetic mineral, not the temperature of the transformation (McClelland-Brown 1982). If a CRM is formed during incorporation of a lithic clast into a pyroclastic deposit, it is possible that the T_b of the new or modified grains is greater than the formation temperature (and possibly greater than the T_{emp}). If this is the case, then it is possible to have two suites of grains with $T_b > T_{emp}$: one primary group carrying the earlier, randomly oriented remanence direction, and a secondary group carrying a remanence in the ambient field direction, such that the T_b values of these groups overlap. One effect of such overlapping T_b spectra is to cause curvature in the vector plots at temperatures above T_{emp} (cf. McClelland-Brown 1982). In such cases the estimate of the high-T_b direction will be biased towards the overprint direction, but this does not affect the estimate of T_{emp}.

Bardot and McClelland (2000) have shown that palaeointensity experiments can be used to assess the origin (pTRM, CRM, or a combination of both) of the low-T_b component. Furthermore, even if alteration has occurred, valuable information can be gained about the characteristics of the magnetic alteration, allowing assessment of the reliability of T_{emp} estimates. However, such experiments are very time consuming and, therefore, in this work we have used measurements of high-temperature susceptibility to assess whether CRM alteration has effected the T_{emp} estimates.

Sampling strategy and techniques

Our sampling strategy was designed to test whether palaeomagnetic temperature estimates are controlled by a number of factors: (1) block size, (2) stratigraphic height in the deposit, (3) clast lithology, (4) radial distance from vent, and (5) azimuth with respect to the vent. To this end, we sampled vertical profiles through the veneer deposit at varying distances from vent, and collected lithics of varying sizes from each location, where possible (sample sites in Fig. 1). Sampling sites were positioned to provide as good an azimuthal and radial spread as possible. Where possible, valley-pond deposits were also sampled in close proximity to the veneer samples, to compare palaeotemperatures of the two facies. Layer 1 deposits were also collected at the same sampling sites as layer 2, where possible. We concentrated on collecting igneous lithic clasts because of the uncertain reliability of pumice temperature estimates (as above), but collected some pumices at most sites. We specifically avoided collecting samples of sedimentary lithics, as these are much more liable to alter chemically when heated, which would make the palaeomagnetic analysis more difficult. We collected 488 lithic clasts which comprised six sub-types of rhyolite, andesite, and one clast of mudstone. Analytical procedures allowed us to sample lithics down to 0.5 cm in diameter, so that the finer-grained, distal parts of the deposit are represented. We also specifically sampled in areas where pink to red thermal-oxidation colours were present, to determine if this colouration was controlled by thermal conditions.

The principal sampling procedure was to take orientated, 0.5–10 cm diameter hand samples (as done by McClelland and Druitt 1989). Both lithic and pumice clasts were oriented by gluing a rigid plastic plate onto the surface of the clast, and marking the strike and dip of this plate. At medial to distal sites, where the diameter of the lithic clasts was very small (down to 0.5 cm), fresh surfaces were cut within the deposits using a spade. Samples were then taken from freshly parted surfaces where the spade had not smoothed or disturbed the deposit. A plastic plate was glued onto the fresh surface, centred onto the chosen clast (although other clasts would also adhere, these were removed later). For >3 cm lithic clasts, standard (2.5-cm diameter) cores were subsequently drilled from the blocks. For 2–3 cm lithic clasts, 1.9-cm-diameter cores were drilled. Samples with a diameter <2 cm were set in 2.5-cm-diameter cylinders made of aluminium oxide dispersed in a sodium silicate solution, which could be considered to be effectively non-magnetic. Magnetization of the samples was measured using either a CCL cryogenic magnetometer or a Molspin spinner magnetometer. Samples were demagnetized, using a furnace with a residual field of <5 nT, in temperature steps of 40 or 50 °C (initial step 80 °C), until the remaining intensity was less than 5% of the NRM. The data were plotted on Zijderveld orthogonal demagnetization diagrams and the principal components of magnetization were analysed using the SuperIAPD programme written by Trond Torsvik, in-
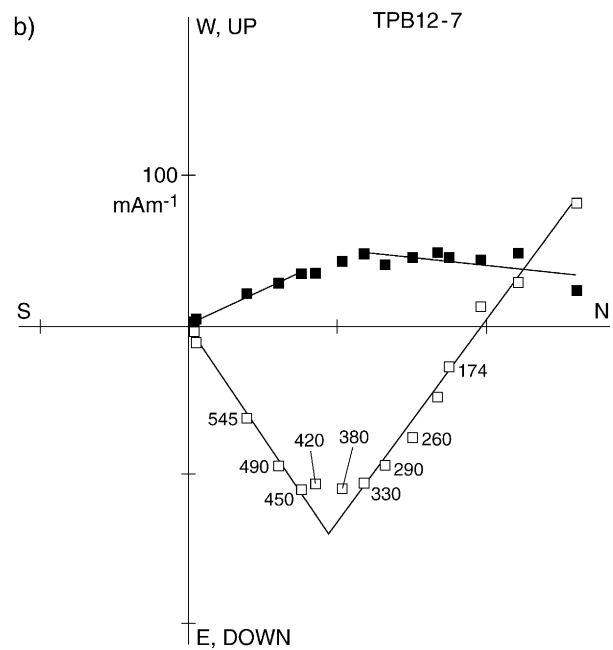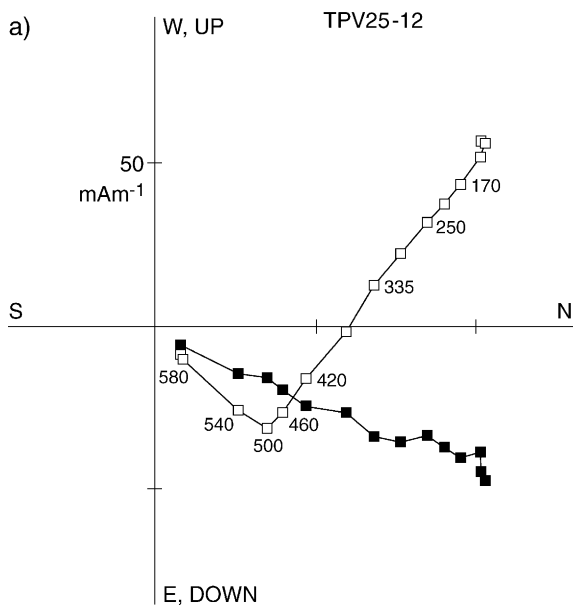
a) TPV25-12

b) TPB12-7

Fig. 3a, b Demonstration of how to interpret sample emplacement temperatures (T_{emp}) from palaeomagnetic data. *Solid squares* show the projection of the magnetization vector for the clast onto the horizontal plane at different laboratory temperatures (in °C); *open squares* show the vertical projection of the same vector at the same laboratory temperatures. **a** Lithic sample with no CRM overprinting gives sharp break between low- and high-temperature components. **b** Lithic clast with some CRM overprinting shows curvature between the low- and high-temperature lines

corporating the LINEFIND algorithm of Kent et al. (1983). The significance of grouping of vector components from each site was assessed using Watson's (1956) test for randomness. Watson defined a parameter R_o (N) which can be used to determine whether a set of N directions is significantly well grouped at the 95% confidence level by comparing it against R, the length of the vector sum of the N components being analysed. R is close to N if all the vectors are in a similar direction; R is small if the directions are randomly distributed. If the value of R (N) exceeds R_o (N), then we are 95% confident that all N magnetization components record the same magnetic field, and are thus contemporary.

To determine T_c, measurements of low-field susceptibility versus temperature were made using a CS-2 attachment to a KLY-2 Kappabridge, using 1–2 cm^3 of powdered sample. Measurements of susceptibility were made every 15–20 s as the sample was heated from room temperature to 700 °C, and then cooled from this temperature to 50 °C. The total time for a 700 °C run was approximately 2 h. Most of the experiments were carried out in an argon atmosphere, to inhibit oxidation. However, as some of the pumice and lithic clasts sampled in this study probably cooled in an oxidizing environment, several experiments were carried out in air to check for differences in behaviour between these two atmospheres.

Results

General features of the data

Lithic clasts

Well-defined emplacement temperatures can be determined from those lithic clasts in which two components of magnetization are identified from thermal demagnetization. In samples where the primary magnetization component of the lithic has been overprinted by thermal activation of the magnetism (pTRM), with no chemical modification to magnetic mineralogy, we find that these two components are delineated by a sharp change in direction during demagnetization. This change of direction takes place at the emplacement temperature. This behaviour is depicted in Fig. 3a for sample TPV25-12. In this example, the initial magnetic vector points upwards and to the northeast. As the thermal demagnetization progresses, the magnetization vector remains north-easterly but progressively shallows in inclination up to the 500 °C step, and then remains in the same direction but decreases in intensity. On the vector plot, these changes in the magnetic vector map out two separate lines; in this case these are best seen in the vertical projection of the data (open symbols). All the points between 0 and 500 °C fall on the same low-temperature line, the direction of which (D=021°, I=−50°) is close to that of the present Earth's field at this locality. Points from 500 °C and higher temperatures fall on the high-temperature line, which passes through the origin and has a direction
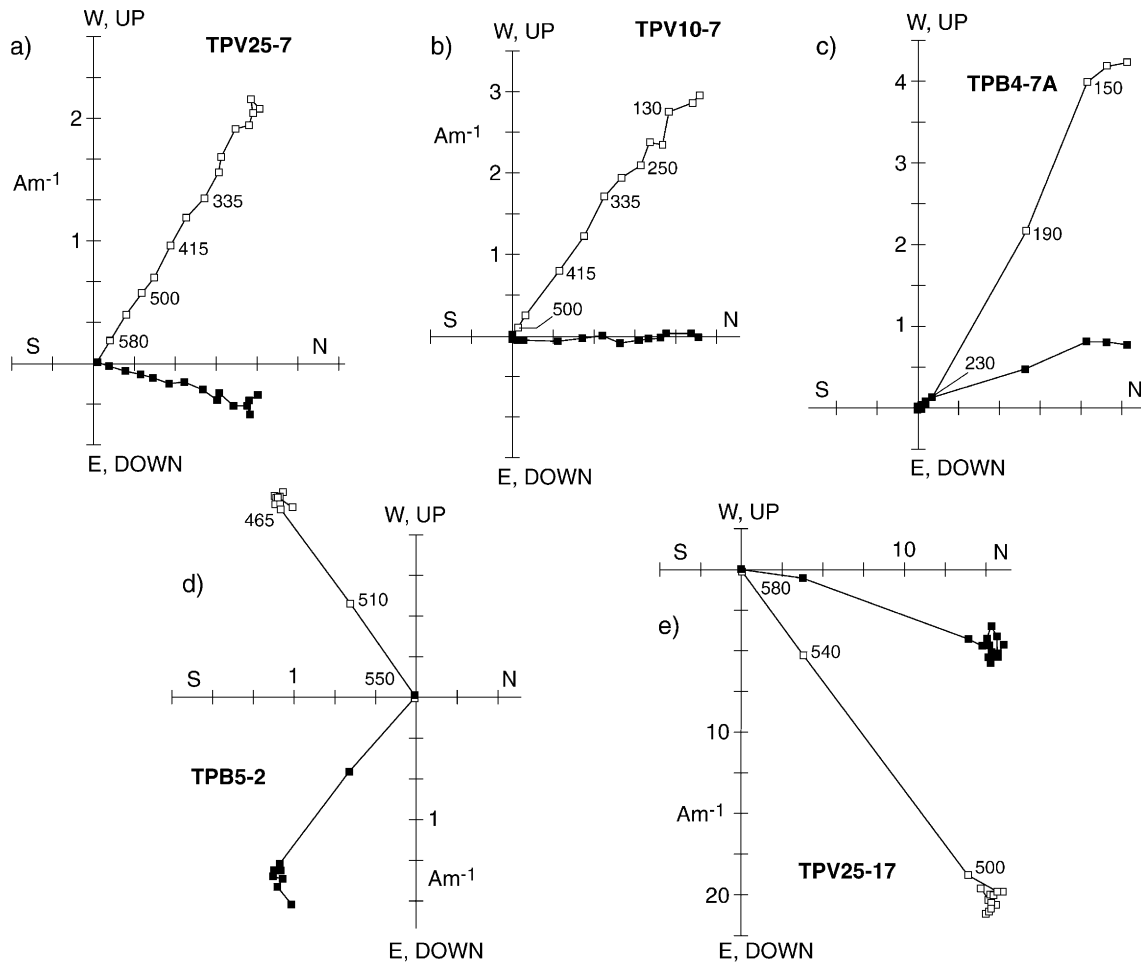
Fig. 4a–e Lithic clasts with single magnetic component. **a–c** Component is in present Earth's field direction and gives minimum estimates of clast emplacement temperature. **d**, **e** Component is in random direction, and low unblocking temperatures are absent; such samples give a maximum estimate of T_{emp}

(D=025°, I=+39°) which is statistically different from the present Earth's field. This line defines the original magnetization direction of the clast, which was moved into a different orientation during transport. We do not take a single temperature as our best estimate, but use the temperature range between the last point on the low-temperature line and the second point on the high-temperature line such that, for our example clast TPV25-12, our best estimate of T_{emp} is 500–540 °C. We call this demagnetization style 'type 1a' behaviour.

In samples where the heating of the lithic clast has caused a chemical modification to magnetic mineralogy, the new remanence which is acquired on cooling in the deposit has two origins. The first is by thermal activation (pTRM), as in the previous example, and the maximum blocking temperature cannot exceed the temperature to which the clast was heated. The second origin is as a CRM carried by new or modified magnetic minerals. As explained above, blocking temperatures of CRM can exceed the temperature at which the reaction takes place, as T_b is controlled by grain size, not reaction temperature. Hence, blocking temperature intervals above the emplace-

ment temperature can contain both the primary non-Earth's field direction plus the new CRM overprint in the Earth's field direction. This gives rise to curvature of the vector plot, as shown in Fig. 3b for sample TPB12-7. Here, data points at temperatures up to 330 °C fall on the low-temperature line (D=004°, I=−54°), sub-parallel to the present Earth's field direction. Data points from 450 °C and above fall on a line (D=335°, I=+53°) which passes through the origin and is significantly different from the present Earth's field. However, points from 380 and 420 °C lie between these two lines, as both low- and high-temperature components are being removed at the same time. In an example with curvature like this, we take T_{emp} as the range defined by the last measured value on the low-temperature line, and the next temperature above this. Thus, for clast TPB12-7, T_{emp} is 330–380 °C. We call this demagnetization style 'type 1b' behaviour.

There are other categories of demagnetization data which allow us to make less-precise, but still useful estimates of emplacement temperature. In some samples, the lithic clast has been heated above the maximum Curie temperature of its magnetic minerals, no trace of the
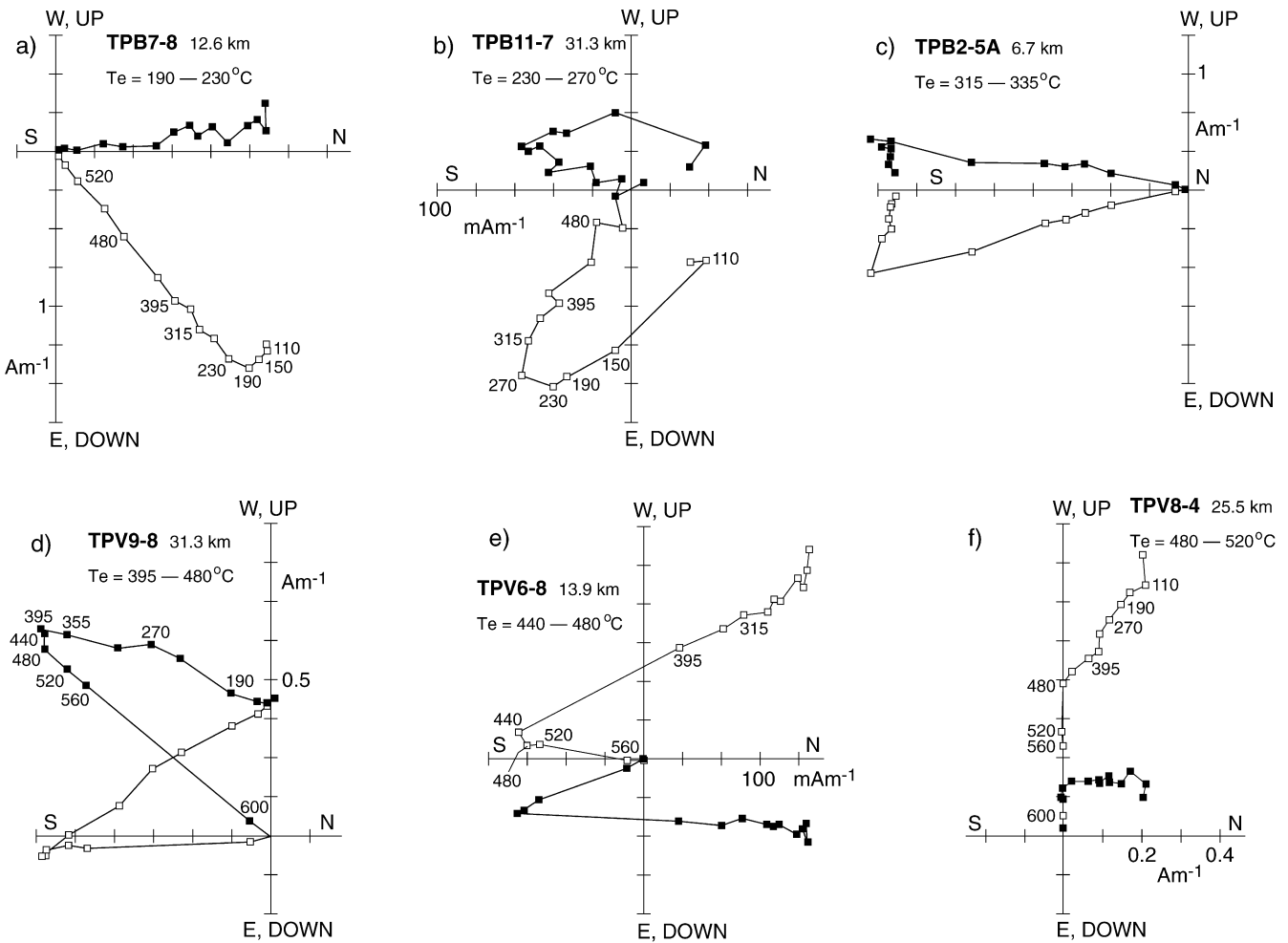
Fig. 5a–f Representative vector plots for selected two-component lithics, indicating distance from vent in km. Symbols as in Fig. 3

original remanence remains, and the remanence is a single component in the present Earth's field direction. In such cases, the emplacement temperature of the clast was greater than the maximum Curie temperature. Figure 4a–c shows three examples of single-component magnetization, illustrating the range of Curie temperatures we observe in single-component samples. Figure 4a shows a single component which is fully demagnetized between 580 and 620 °C for sample TPV25-7. Figure 4b shows a single component which is demagnetized between 500 and 540 °C. Finally, Fig. 4c illustrates an unusually low Curie temperature clast where only 1% of remanence is left by heating to 355 °C. In these examples, we define the emplacement temperature as >580 °C, >500 °C and >355 °C respectively. We call this demagnetization style 'type 2' behaviour.

In some other samples, the natural magnetic grain-size distribution has a more-restricted range than normal, and there are no grains present with low blocking temperatures (Fig. 4d, e). When the clast has been emplaced at a temperature which is less than the relevant minimum blocking temperature, then no thermal overprint can be imprinted and so no record of the heating event is obtained. Figure 4d shows sample TPB5-2, where no demagnetization occurs during demagnetization up to 430 °C and most demagnetization takes place in two steps at 510 and 550 °C. Figure 4e shows a similar sample TPB6-5, where demagnetization only occurs between 505 and 590 °C. In these two examples, we define the emplacement temperature as <430 °C and <505 °C respectively. We call this demagnetization style 'type 3' behaviour.

In all, 488 lithic samples were thermally demagnetized. All samples display either a one- or two-component remanence, and representative vector plots are displayed in Fig. 5. Almost all lithic samples respond stably to thermal demagnetization and yield well-defined vector trajectories. Most samples behave as types 1a, 2 or 3, as follows. Two-component magnetizations (type 1a) are usually separated by a sharp change in direction on the vector plot, with the low blocking temperature component parallel to present Earth's field and the high blocking temperature component in a random direction. Single-component magnetizations with well-distributed blocking temperature spectra (type 2) are usually parallel to present Earth's field, while samples where low blocking tem-

perature grains are absent (type 3) have single-component magnetizations in a random direction. Only a small proportion of the samples show type 1b behaviour with curvature between low- and high-Tb components. This gives us a high degree of confidence in the reliability of our emplacement temperature estimates.

We find a few samples which have a single component of magnetization which is in a random direction but with a well-distributed blocking temperature spectrum which should have acquired a remanence component parallel to the Earth's field on cooling after emplacement. We also find a few samples with two components where neither the low- nor the high-temperature component is parallel to the present Earth's field. We have interpreted these data as representative of clasts which had moved in the deposit prior to our sampling, and do not include them in the temperature analysis.

We have grouped low-Tb components from types 1a and 1b samples together with directions of type 2 samples for each site in Table 2. Statistically, the low-Tb remanences for all the Taupo deposits are significantly grouped and lie close to the present-day Earth's field direction for Lake Taupo, with declination 22.5° and inclination −64°. This indicates that the low-Tb components of the lithic clasts were acquired while cooling in situ in the deposit. We have grouped high-Tb components from type 1 samples together with directions from type 3 samples for each site. Statistically the high-Tb remanences for most of the Taupo deposits are randomly grouped, indicating that this component predates emplacement.

Pumice clasts

In all, 123 pumice samples were thermally demagnetized; representative vector plots and intensity decay graphs are displayed in Fig. 6. The directions carried by these pumice clasts are single-component, and lie close to the present Earth's field direction. The maximum temperature to which this remanence persists is variable, and Fig. 6a, b illustrates an example where remanence persists up to 570 °C, while Fig. 6c, d shows a sample where the remanence has decayed to less than 10% of initial value by 315 °C. This temperature is referred to as the maximum unblocking temperature, T_{ub}, in a following section.

Rock-magnetism results

Spurious emplacement temperature estimates may result from a situation where a change in magnetic chemistry of a lithic clast occurred during a low-temperature emplacement process which created significant amounts of a new magnetic mineral with low or intermediate values of T_c. For example, consider a flow with a true equilibrium temperature of 150 °C, a lithic clast with an original magnetite mineralogy (T_c=580 °C), and new formation of titanomagnetite with T_c=300 °C. The new titanomagnetite will all be magnetized in the direction of the present Earth's magnetic field, and will not be demagnetized until 300 °C. The original magnetite will have a thermal overprint to 150 °C and will carry the original, now random magnetization direction in blocking temperatures between 150 and 300 °C. This situation will simply result in curvature of the vector plot between 150 and 300 °C, if the amounts of the original and new magnetic minerals are similar. However, if the remanence of the new phase is dominant, then the overprint in the present Earth's field direction will persist up to 300 °C and a spuriously high emplacement temperature will be estimated.

To test for this possibility, we have determined the range of T_c values using the variation of susceptibility with temperature in 34 lithic samples, to see if emplacement temperature estimates from lithic clasts are coincident with dominant T_c values. Susceptibility drops to zero at $T=T_c$ for a mineral, and we determine the dominant T_c value by extrapolating the maximum slope to the axis, as shown in Fig. 7a. We find that most lithic samples are dominated by a magnetite or low-titanium magnetite with T_c values between 540 and 580 °C. Figure 7 shows five examples of lithic emplacement temperatures ranging from 160–230 to 500–540 °C which all contain similar magnetite mineralogy, indicating that the emplacement temperatures are valid. This is typical of lithic material from the Taupo ignimbrite. Some lithic samples do contain multiple magnetic minerals, which are identified by several sharp decreases in susceptibility at various temperatures (e.g. Fig. 7k, l). However, we do not find any coincidence between emplacement temperature and Curie temperature, as all the two-mineralogy samples we have identified only have one magnetization direction and have not yielded emplacement temperature estimates. This lack of coincidence adds support to the validity of our emplacement temperature estimates.

We also investigated the variation of susceptibility with temperature in 31 pumice samples; typical examples are shown in Fig. 8. Comparisons were made between magnetic behaviour when pumice samples were heated in air and when heated in argon to prevent oxidation reactions occurring. When samples were heated in argon, the magnetic susceptibility shows a single T_c value on the heating run, defined by a reasonably sharp drop of susceptibility towards zero (e.g. TPB13-12). The cooling run shows chemical alteration has occurred during heating in the laboratory up to 700 °C as the original T_c has reduced slightly, and susceptibility now exists at higher temperatures than on the heating cycle. When heated in air, the same sharp decrease is seen on the heating run, but there is always a tail which smears the susceptibility to higher temperatures (e.g. TPB22-11 and TPV20-3A). We interpret this as evidence for maghemitization (oxidation) during the laboratory heating experiment, which is inhibited in the early part of the heating cycle in argon but still occurs at high temperature, so that the effects are thus seen on cooling in argon. Because of this, we take the initial onset of a susceptibility drop as indicative of the dominant Curie temperature, as indicated in Fig. 8.

Table 2 Statistics of magnetization components for lithic clasts from the Taupo ignimbrite

Site	Low-T$_b$ component								High-T$_b$ component							
	N[a]	k	α_{95}	Mean dec.	Mean inc.	R	R$_o$	Random?	N	k	α_{95}	Mean dec.	Mean inc.	R	R$_o$	Random?
TPB1	9	15.7	13.4	1.3	−53.7	8.5	4.76	No	8	1.4	79.6	27.6	−18.9	3.2	4.48	Yes
TPB2+3	14	19.5	9.2	5.3	−57.2	13.3	5.98	No	13	1.2	88.4	358.1	−3.5	2.9	5.75	Yes
TPB4	7	12.5	17.7	354.4	−50.5	6.5	4.18	No	7	2.1	56.5	348.9	−35.2	4.1	4.18	Yes
TPB5	4	10.8	29.4	345.3	−50.6	3.7	3.10	No	4	1.3	>90	325.0	−23.4	1.7	3.10	Yes
TPB6	7	48.3	8.8	0.5	−55.4	6.9	4.18	No	6	1.2	>90	16.8	−13.5	1.9	3.85	Yes
TPB7	6	35.1	11.5	356.8	−52.2	5.9	3.85	No	6	1.7	76.2	348.9	−12.6	3.1	3.85	Yes
TPB8	28	16.6	6.9	0.0	−50.9	26.4	8.54	No	25	1.2	66.6	348.4	3.0	4.5	8.07	Yes
TPB9+10	3	11.4	38.4	4.5	−39.0	2.8	*	*	3	3.4	82.1	358.0	−42.5	2.4	*	*
TPB11	4	35.8	15.6	6.6	−53.3	3.9	3.10	No	4	2.1	87.2	29.0	32.1	2.6	3.10	Yes
TPB12	9	32.0	9.2	357.8	−52.0	8.8	4.76	No	9	1.3	87.8	4.9	−0.5	2.9	4.76	Yes
TPB13	7	28.4	11.5	25.6	−43.9	6.8	4.18	No	7	2.0	60.2	356.7	19.3	3.9	4.18	Yes
TPB14	6	26.3	13.3	13.1	−56.0	5.8	3.85	No	3	2.7	>90	353.3	−34.1	2.3	*	*
TPB15	4	61.0	11.9	1.5	−50.7	4.0	3.10	No	4	1.6	>90	350.1	−9.2	2.1	4.18	Yes
TPB16	4	25.8	18.5	356.8	−56.6	3.9	3.10	No								
TPB17	8	27.1	10.8	354.7	−56.1	7.7	4.48	No	3	6.7	51.9	354.7	−9.7	2.7	*	*
TPB18	8	89.8	5.9	9.9	−56.9	7.9	4.48	No	3	4.2	69.8	37.7	−24.0	2.5	*	*
TPB19	8	20.4	13.7	0.5	−49.3	6.7	4.48	No								
TPB20	7	21.6	13.3	3.7	−41.8	6.7	4.18	No	5	1.57	>90	142.6	−68.9	2.4	3.50	Yes
TPB21	8	10.3	18.1	18.7	−48.1	7.3	4.48	No	5	1.32	>90	133.9	−28.1	1.9	3.50	Yes
TPB22	4	20.6	20.7	11.5	−62.9	3.9	3.10	No	3	0.9	>90	0.7	11.1	0.8	*	*
TPV1	6	11.5	20.7	34.7	−53.1	5.6	3.85	No	5	1.3	>90	356.6	−2.8	1.9	3.50	Yes
TPV2	5	12.5	22.5	347.5	−58.5	4.7	3.50	No	5	1.1	>90	346.2	7.4	1.2	3.50	Yes
TPV3	3	7.3	49.6	352.2	−52.6	2.7	*	*	3	5.5	58.6	341.2	48.7	2.6	*	*
TPV4	4	4.7	47.7	9.0	−46.3	3.4	3.10	No	4	1.3	>90	329.3	−20.5	1.7	3.10	Yes
TPV5	2	291.8	14.7	358.1	−50.0	2.0	*	*	2	1.2	>90	359.8	9.1	1.2	*	*
TPV6	15	14.0	10.6	13.0	−43.3	14.0	6.19	No	13	1.2	82.1	12.2	−13.0	3.2	5.75	Yes
TPV7	6	17.9	16.3	1.4	−50.5	5.7	3.85	No	6	1.0	>90	337.7	5.6	0.9	3.85	Yes
TPV8	17	9.7	12.1	4.6	−38.6	15.4	6.60	No	16	1.5	50	285.9	−62.5	6.0	6.40	Yes
TPV9	4	12.7	26.9	45.1	−34.1	3.8	3.10	No	4	1.3	>90	32.5	−14.2	1.7	3.10	Yes
TPV10	8	85.4	6.0	0.1	−50.4	7.9	4.48	No	5	1.3	>90	356.3	−17.5	2.0	3.50	Yes
TPV11	9	60.8	6.7	359.5	−52.3	8.9	4.76	No	3	1.1	>90	5.8	−11.1	1.1	*	*
TPV12	5	23.5	16.1	348.9	−61.8	4.8	3.50	*								
TPV13	7	6.7	25.2	3.4	−54.6	6.1	4.18	No								
TPV14+15	16	39.7	5.9	356.4	−56.6	15.6	6.40	No	4	1.3	>90	252.8	−53.4	1.7	3.10	Yes
TPV16	9	12.7	15.0	1.4	−54.7	8.4	4.76	No	2	16.8	65.5	358.5	−67.2	1.9	*	*
TPV17	9	59.3	6.7	9.2	−57.5	8.9	4.76	No	6	1.2	>90	38.3	−4.6	1.7	3.85	Yes
TPV18	9	34.7	8.9	1.7	−47.7	8.8	4.76	No	5	1.0	>90	000.0	−1.4	1.0	3.50	Yes
TPV19	7	21.8	13.2	353.3	−53.5	6.7	4.18	No	4	1.4	>90	3.7	−22.0	1.8	3.10	Yes
TPV20	7	24.1	12.6	350.7	−54.3	6.8	4.18	No	2	0.7	>90	311.5	4.5	0.5	*	*
TPV21	7	12.3	17.9	5.6	−53.8	6.5	4.18	No	2	30.6	46.8	16.0	−20.4	2.0	*	*
TPV22	11	18.4	10.9	348.7	−51.9	10.5	5.29	No								
TPV23	8	15.2	14.7	359.8	−53.3	7.5	4.48	No								
TPV24	6	15.5	17.6	8.7	−52.3	5.7	3.85	No	3	1.2	>90	9.6	12.6	1.3	*	*
TPV25	13	11.5	12.8	9.6	−51.0	12.0	5.75	No	8	1.6	69.0	4.6	3.4	3.6	4.48	Yes

[a] N, number of samples; k, best estimate of the precision parameter; α_{95}, 95% confidence limit; mean dec., declination of the mean direction of magnetization of N vectors; mean inc., inclination of magnetization; R, vector resultant of N vectors; R$_o$, Watson's parameter; grouping is random for N vectors if R<R$_o$; asterisk *, data are too few to calculate accurate statistical parameters (N<4)

Fig. 6a–d Representative vector plots and intensity decay curves for selected pumices, indicating distance from vent in km. Symbols as in Fig. 3. **a**, **b** High unblocking temperature pumice. **c**, **d** Low unblocking temperature pumice
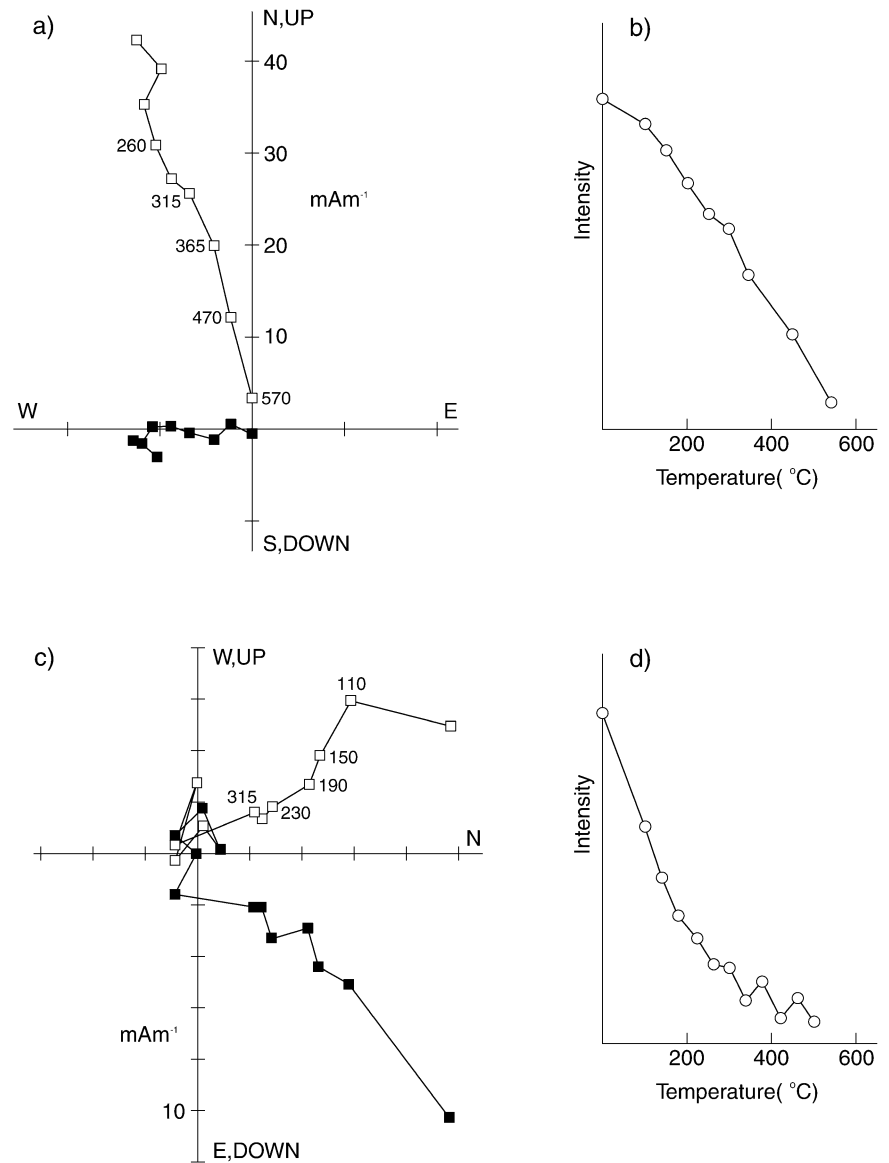
Bahar et al. (1993) reported emplacement temperatures derived from pumices from the Taupo ignimbrite, which varied from 220–300 °C at proximal sites to 450–580 °C at distal sites. In order to test these results, we used 31 pumice samples, chosen to have a range of behaviour on thermal demagnetization. Our samples range in behaviour from those where the remanence component is clearly defined up to 580 °C (which would be taken to indicate emplacement at >580 °C, using the Bahar et al. (1993) methodology), to samples where the remanence can only be defined up to 200–300 °C and unstable magnetic behaviour occurs above these temperatures (which would be taken to indicate low emplacement temperatures using the Bahar et al. (1993) methodology). Values of T_c are compared to maximum blocking temperatures for these samples in a following section.

Emplacement temperatures and their interpretation

Individual clast emplacement temperatures (T_{emp}) are determined from the lithic clasts as described above. Types 1a and 1b samples provide quantitative emplacement temperature estimates. Type 2 samples were emplaced above the T_c of the magnetic minerals present, which therefore provides a minimum estimate of T_{emp}. Magnetite or Ti-poor titanomagnetite are the main remanence carriers for most of the samples in this category, but several samples are dominated by Ti-rich titanomagnetite (see section above) with T_c values of 200 to 350 °C. The remanence of type 3 samples only unblocks above a certain temperature and these clasts can be used to infer maximum estimates of T_{emp}. These temperature estimates for individual samples are shown in Fig. 9 for representative sites from layers 1 and 2 of the Taupo ignimbrite.

McClelland and Druitt (1989) considered the thermal histories of lithic clasts emplaced with a range of
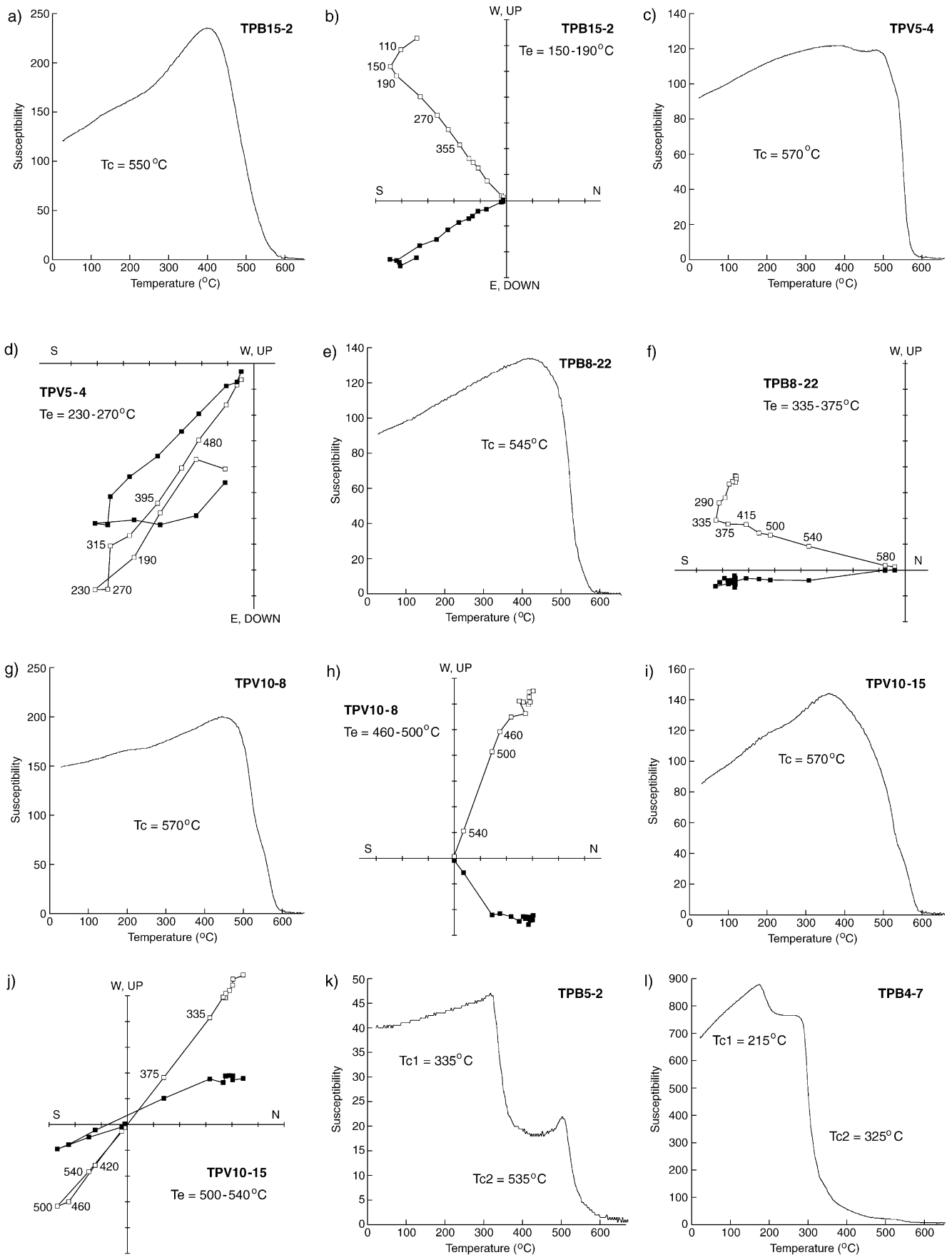
504

Fig. 7a–l Variation of magnetic susceptibility with temperature for selected lithics from the Taupo ignimbrite (heating curve only), and vector plots giving sample emplacement temperature estimates for five of the same samples

Fig. 8a–f Variation of magnetic susceptibility with temperature for selected pumices from the Taupo ignimbrite. *Full curve* indicates heating and *dashed curve* shows cooling
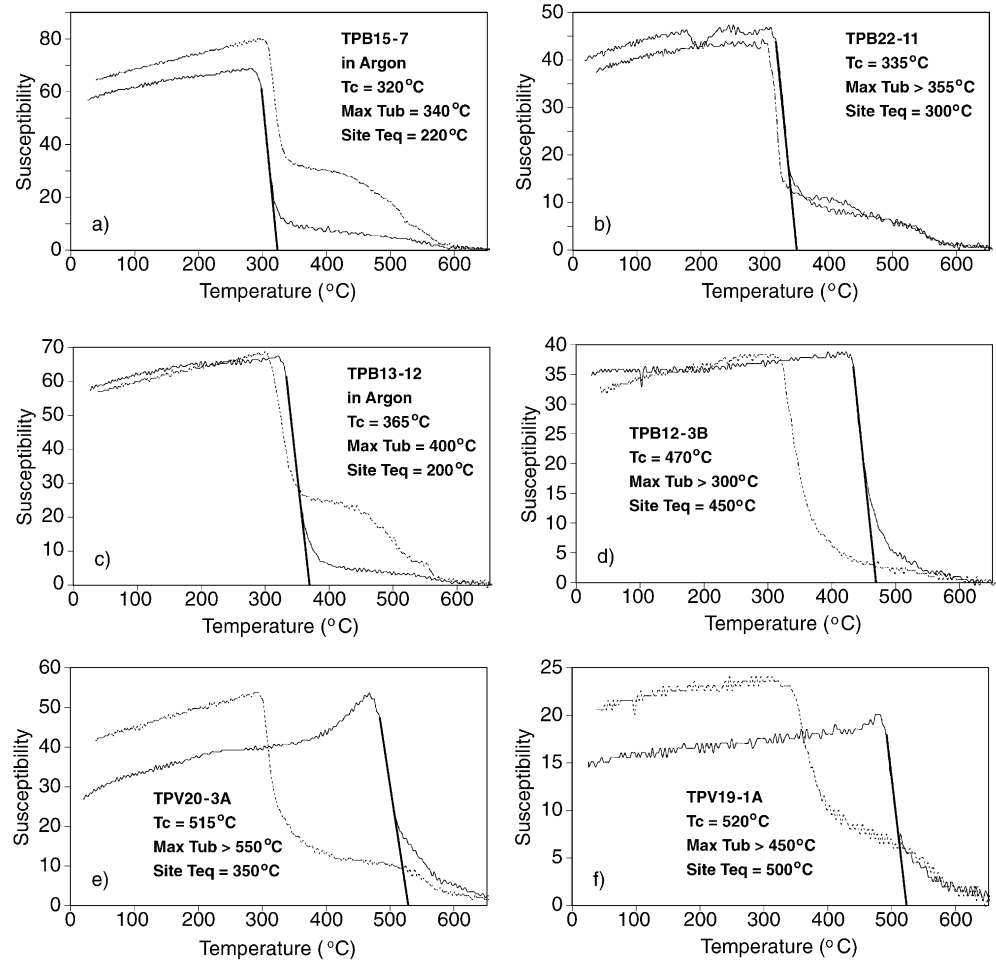

temperatures. As the host deposit cools, individual clasts will either heat up or cool down to some average temperature due to heat transfer. Under normal conditions, lithics with an initial temperature greater than the average temperature would cool with time after emplacement, and all the grains with T_b values less than the initial temperature will be remagnetized. Clasts with initial temperatures less than the average temperature will heat up to the average temperature before cooling to ambient, so that remagnetization of all the grains with T_b values less than the average temperature will occur. Lithic clasts in a pyroclastic deposit therefore will record T_{emp} values ranging from the average temperature of the deposit at emplacement to the maximum initial temperature of a clast, which may exceed T_c (580 °C for magnetite). Thus, an average or equilibrium temperature (T_{eq}) of a deposit is most closely approximated by the lowest value of T_{emp} at a particular location. The deposit takes time to equilibrate and therefore the T_{eq} of a deposit represents a minimum estimate of the T_{emp} of the whole deposit upon deposition. The best estimate of T_{eq} at each site is illustrated by a horizontal dotted line in Fig. 9. Cooling-rate corrections have been applied to the best estimate of T_{eq} at each valley-pond ignimbrite site, to allow for the difference

between laboratory and natural timescales, and are tabulated in Table 3.

There are data from lithics recording significantly higher temperatures in the proximal deposits than the inferred T_{eq} value (e.g. Fig. 9a, valley-pond deposit at 13.9 km from vent). We have sampled six sub-types of rhyolite and one type of andesite clast, and we find that representatives of each lava type record these higher temperatures, so that there is no evidence for a specific high-temperature source region. Such anomalously hot clasts are most easily interpreted as representing lithics which had undergone a previous heating event from which they had not cooled before incorporation in the deposit. Our preferred explanation for this is that the lithics were originally incorporated in ignimbrite which accumulated around the vent at the time of earlier plinian fall activity (Table 1; the early ignimbrite flow units of Wilson and Walker 1985), and were disrupted and incorporated into the climactic outburst. The early ignimbrite flow units are locally incipiently welded where now exposed on land, and so any incorporated lithics are likely to have been heated up to close to or somewhat above the Curie point for magnetite (580 °C). The lithic clasts are unlikely to have been eroded from the land surface at considerable distance from vent during trans-

Fig. 9a–d Range of clast emplacement temperature (T_{emp}) for four representative sites. Site equilibrium temperature (T_{eq}) is determined from the minimum sample emplacement temperature and is shown as *horizontal dotted line*. **a**, **c** Site TPV6 and TPV3; estimated T_{eq} of 180 °C. **b** Site TPV8; estimated T_{eq} of 220 °C. **d** Site TPV25; estimated T_{eq} of 460 °C
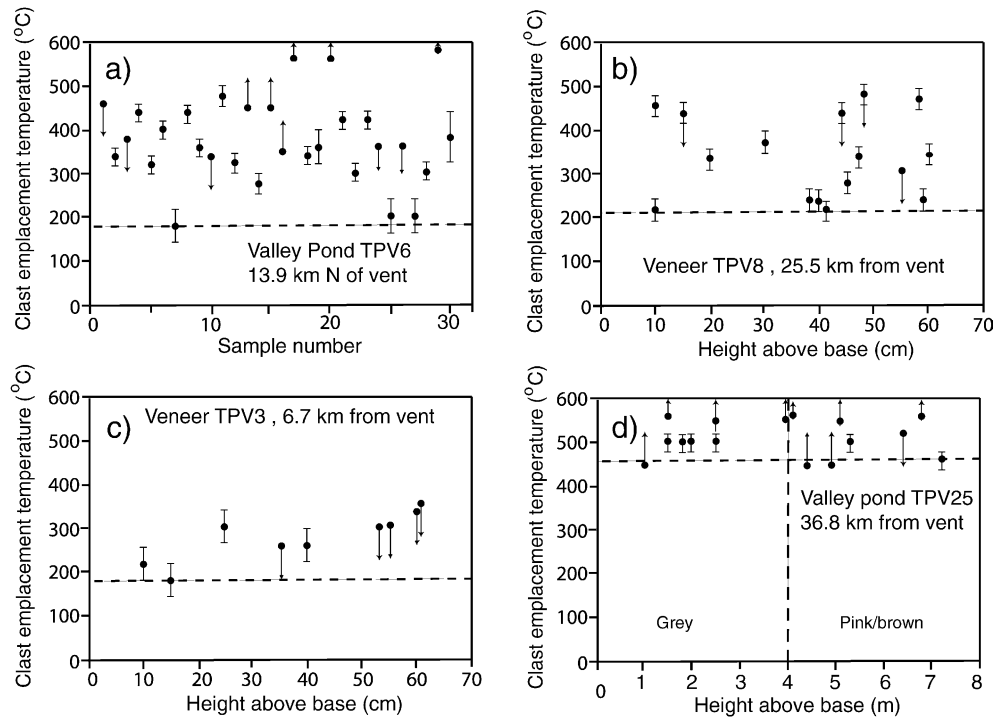
Temperature structure of the Taupo ignimbrite

Lithic data

Our best estimates of site equilibrium temperatures, T_{eq}, for lithics from layer 1 show a distinct variation with distance from vent (Fig. 10a). At proximal localities, layer 1 is dominated by lithics emplaced at 150–300 °C, and clasts emplaced above 580 °C (i.e. T^c) are uncommon whereas at medial to distal localities (>40 km), layer 1 is dominated by lithics emplaced at $T>T^c$ and displays minimum site temperatures of 300–500 °C. The T_{eq} of layer 1 is approximately 200 °C up to a distance of 37 km from vent, whereas beyond 46 km from vent the T_{eq} of layer 1 is >400 °C, apart from the furthest locality which has a T_{eq} of 310 °C (see Fig. 10a). There is no significant difference in T_{eq} between the two layer 1 facies, despite their contrast in lithic abundances.

Values of site equilibrium temperatures, T_{eq}, for lithics from layer 2 show a parallel variation to layer 1 with distance from vent (Fig. 10b). Proximal localities are dominated by low-temperature lithics (150–250 °C), whereas medial to distal localities (>37 km) are dominated by clasts emplaced above 580 °C (i.e. T_c). The T_{eq} of layer 2 is approximately 200 °C up to a distance of 31 km from vent, whereas beyond 37 km from source the T_{eq} of layer 2 is >400 °C. At localities where both layers 1

and 2 were sampled, site equilibrium temperatures for the two layers are very similar (see Table 3), the only difference being that the increase in T_{eq} for layer 1 occurs between localities 37 and 46 km from vent, whereas for layer 2 the increase occurs between 31 and 37 km. The veneer deposit and valley-ponded ignimbrite in layer 2 also display similar thermal characteristics (see Fig. 10). Samples from many of the sites studied come from vertical profiles through the layer 1 or 2 deposits. We find no evidence for thermal gradients preserved within the deposits (e.g. Fig. 9b–d).

From the lithic data, both layers 1 and 2 of the ignimbrite display consistent variations in T_{eq} values between proximal and medial/distal localities, with the former being cooler. The question then arises—could these differences be an artefact of alteration producing falsely high T_{eq} estimates in medial/distal regions? Our rock-magnetic data show no correlation between intermediate emplacement temperatures for individual clasts and the Curie temperature of a magnetic phase, which allows us to conclude that alteration has not adversely affected our estimates of individual sample emplacement temperature or site equilibrium temperature.

Wilson (1985) documented a change in colour of the pumices from the typical pale cream to a pink, red or purple colouration in medial to distal zones, indicated in Fig. 11. This pink colouration has been interpreted as being due to thermal oxidation of iron oxides as a result of prolonged exposure to elevated temperatures. We have superimposed our site equilibrium temperatures for layer 2 onto the pink pumice zones, and seven of the eight sites with $T_{eq}>450$ °C show thermal-oxidation colours (Fig. 11).

Table 3 Estimated site mean equilibrium temperature (T_{eq}) of layer 1 lithic- (1H) and pumice- (1P) rich and layer 2 (valley pond (VPI) and veneer (IVD)) deposits, including the amount of cooling-rate correction for VPI, and the final corrected VPI temperatures

Site no.	Distance from vent (km)	T_{eq} layer 1H (°C)	T_{eq} layer 1P (°C)	T_{eq} IVD (°C)	T_{eq} VPI (°C)	Cooling-rate corr. (°C)	T_{eq} VPI corrected (°C)
TPB2	6.7	250					
TPB3	6.7	250					
TPV3	6.7			180			
TPV1	7				200	−50	150
TPB1	8.2	150					
TPV4	9.8			150			
TPV5	10.7			150			
TPB4	10.7	150					
TPB5	11.8	200					
TPV7	12				200	−50	150
TPB7	12.6	150					
TPV6	13.9				180	−50	130
TPV2	15.5				180	−50	130
TPB9	18.4		150				
TPB10	18.4	250					
TPB6	23.1	250	250				
TPB8	25.5	200					
TPV8	25.5			220			
TPB15	26.9		220				
TPB11	31.3		200				
TPV9	31.3			240			
TPB13	32.9		200				
TPV25	36.8				460	−23	437
TPB12	37	200	200				
TPV20	39.9				350	−43	307
TPB17	45.5	300					
TPV11	47.2				450	−26	424
TPV10	47.4				480	−18	462
TPV16	47.5				500	−11	489
TPV19	48.8				500	−11	489
TPB14	49.1		450				
TPV14	49.7			450			
TPV15	49.8				500	−11	489
TPB16	49.8		500				
TPB21	50.9	400	400				
TPV23	50.9			500			
TPB22	50.9	300					
TPV24	50.9			400			
TPB19	52		450				
TPV21	52			480			
TPV12	54				450	−26	424
TPV22	54.1				400	−36	364
TPV18	54.3				425	−33	392
TPB18	54.3	350	350				
TPV13	57			300			
TPV17	63.2			350			
TPB20	79.5	300	300				

Can emplacement temperatures be estimated from pumice data?

In pumice clasts, emplacement temperatures are equal to the maximum unblocking temperature (T_{ub}) of remanence if there has been no post-emplacement alteration of the magnetic minerals, as discussed above. If this is the case, then the T_c of the magnetic minerals in the clast will be significantly greater than the maximum unblocking temperature of the remanence.

Superficially, our pumice data show crudely systematic relationships between maximum T_{ub} values and distance from vent. Proximal sites generally have an abundance of clasts with non-Earth's field component, together with fewer clasts with an Earth's field component which extends to between 200 and 450 °C, and no clasts with an Earth's field component which extends to 580 °C. The medial/distal sites, in contrast, are dominated by clasts with an Earth's field component which extends to 580 °C.

To test whether the relationship between maximum T_{ub} values and distances from vent is robust, we plot T_c against maximum T_{ub} in Fig. 12a, using samples where the maximum value of T_{ub} could be precisely estimated. The data points lie close to the 1:1 line indicated on the graph; a best-fit line has a slope of $T_c=0.94\,T_{ub}$ with $R^2=0.930$. Horizontal bars indicate data from samples
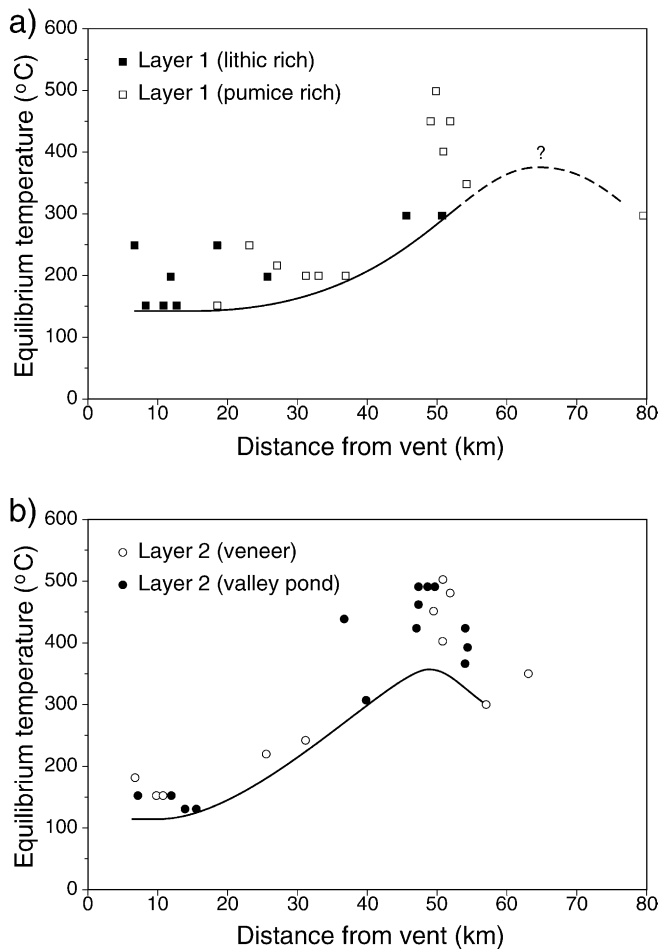
508

a)

b)

Fig. 10a, b Variation of site equilibrium temperature (T_{eq}) with distance from vent for **a** layer 1, and **b** layer 2. The *curved line* on each plot indicates the best estimate of flow temperature variation with distance from vent

Fig. 11 Map of spatial variation of site equilibrium temperature (T_{eq}) from layer 2 deposits; pink thermal pumice oxidation zone shown by *shaded area*

where the unblocking temperature could not be precisely determined due to the onset of unstable demagnetization behaviour, indicating significant chemical alteration of the magnetic minerals in the pumice, which began before laboratory demagnetization was complete. The bar is drawn between the maximum temperature at which the remanence is stable and 580 °C. The true maximum T_{ub} will lie within these bounds (and probably closer to the lower end of the temperature range), and these bounds encompass or lie close to the 1:1 line indicated. This indicates that there is a close-to 1:1 correlation between T_c of the dominant magnetic mineral in the pumice clasts and the maximum unblocking temperature determined from thermal demagnetization. This shows that the maximum unblocking temperature value is not indicative of the emplacement temperature, but is a function of the magnetic mineralogy of the sample.

To test this further, we have plotted pumice clast T_c values against distance from vent (Fig. 12b) and site equilibrium temperature obtained from lithic-clast data (Fig. 12c), to see if there are significant relationships
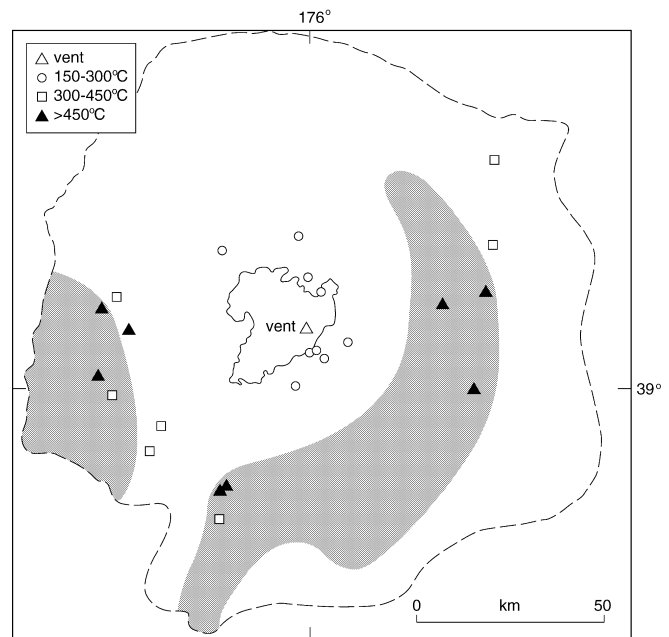
between these data. We find that pumice Curie temperature is not well correlated to distance from vent, as the best-fit line has an R^2 value of only 0.193. So, although there is a superficial indication that maximum T_{ub} of pumice remanence increases away from vent, mirroring the increase in T_{eq} seen in the lithic data (and leading Bahar et al. (1993) to infer an increase in emplacement temperature from the pumices alone), this relationship is not supported by this more-detailed study.

Pumice T_c values are somewhat better correlated to site equilibrium temperatures, although the R^2 value is only 0.465. Our interpretation of this relationship is that the magnetic mineralogy of all pumices was identical at magmatic crystallization temperatures, and would have been a homogeneous titanomagnetite ($Fe_{3-x}Ti_xO_4$) with x~0.5 with a T_c value of about 300 °C. We conclude that where the deposits were emplaced at relatively high temperatures (>350 °C), high-temperature in-situ oxidation after emplacement led to the breakdown of the original titanomagnetite into lamellar intergrowths of low-titanium magnetite (Fe_3O_4) and ilmenite ($FeTiO_3$), thus increasing the effective Curie temperature and leading to an acquisition of CRM remanence in the magnetite lamellae. The initial composition has been retained at the sites where the deposits were emplaced at relatively cool temperatures (<300 °C) and the pumices were cooled relatively rapidly.

Thus, the answer to the question posed in the heading of this section is—no, emplacement temperatures, at least in this example, cannot be determined by thermal demagnetization of pumice remanence. Furthermore, evidence from other studies suggests that this is a more generally applicable statement. Pumices are susceptible to

Fig. 12a–c Variation of pumice Curie temperature with **a** maximum unblocking temperature, T_{ub}, of remanence in same clast; *triangles* indicate clasts where T_{ub} could be precisely estimated; the minimum end of each *horizontal bar* indicates where unstable magnetic behaviour began, the maximum being set at 580 °C; the *straight line* shows a 1:1 ratio; **b** distance from vent; data are very poorly correlated, with $R^2=0.193$ for best-fit line; **c** site equilibrium temperature (T_{eq}); data are poorly correlated, with $R^2=0.465$; best fit shown as *dotted line*, 1:1 ratio shown as *solid line* for comparison
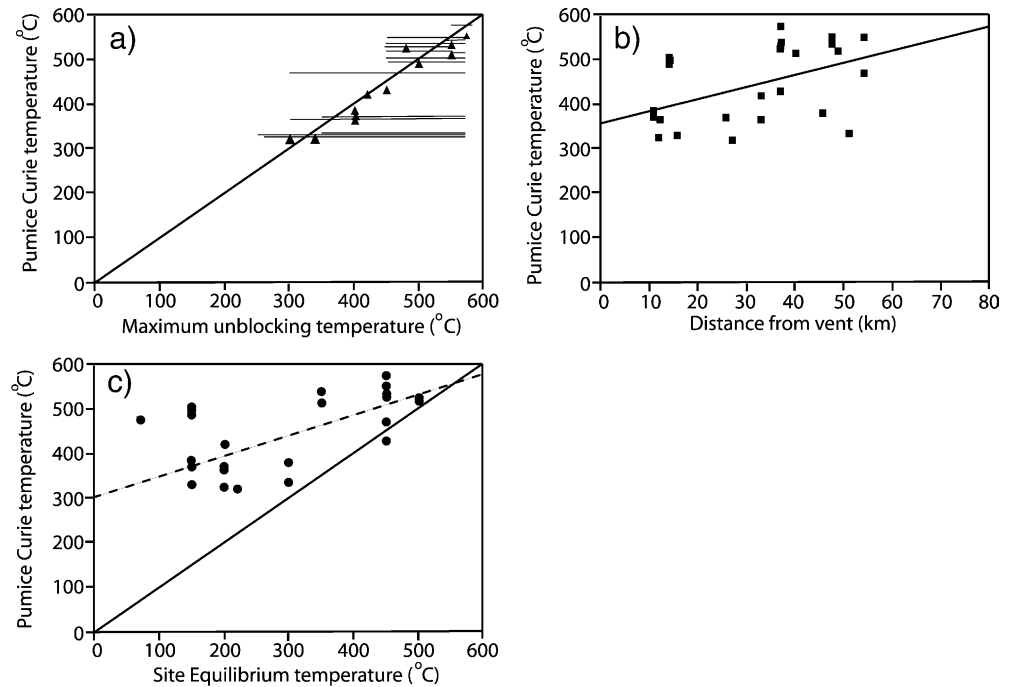
alteration (either during or after deposition) which can produce a CRM which may extend up to the T_c values of the magnetic minerals present, and so give the appearance that the deposit was emplaced hot (e.g. McClelland and Druitt 1989; Donoghue et al. 1999).

Discussion

Interpretations of palaeotemperature data in the Taupo ignimbrite

The palaeomagnetic temperature data presented here allow us to differentiate between the various existing models for the emplacement of the Taupo ignimbrite. There are three main elements of the palaeotemperature data which need to be explained by a viable model, and these are listed below.

Element a

Proximal palaeotemperatures are estimated to be cool (~150 °C up to about 30 km), temperatures rise in the medial region, and are high (>400 °C) in distal zones at 40–50 km. Beyond 60 km from vent, only sparse palaeotemperature data are available but they show a reversion to intermediate values (Fig. 10).

The cooler palaeotemperatures recorded for the more-proximal ignimbrite are broadly consistent with field observations. In several areas around the lake, portions of the ignimbrite contain uncharred (or scorched) wood, or tree-moulds (where the incorporated wood was unaltered and has subsequently rotted), and the ignimbrite matrix is locally vesicular, indicating the presence of trapped steam

bubbles in a partly water-bearing matrix (i.e. T_{eq}~100 °C; Wilson 1985, and unpublished observations). Furthermore, the rock-magnetic analysis of proximal pumice clasts is consistent with rapid quench-cooling of proximal pumices.

Our highest (>450 °C) temperature estimates coincide closely with the presence of pronounced thermal-oxidation colours in the ignimbrite (our Fig. 11; Wilson 1985, Fig. 28). Furthermore, the rock-magnetic analysis of distal pumice clasts indicates post-depositional high-temperature oxidation of primary titanomagnetites. The areal and radial distributions of these high-temperature zones are asymmetric, and such asymmetries are also seen in parameters such as pumice bulk densities and the crystal:lithic ratios in the ignimbrite (Wilson 1985, Fig. 67).

Element b

There is close coherence within and between the individual datasets for layer 1 and layer 2 deposits for data obtained from up to 25 km from vent. This occurs regardless of the content of lithic material (e.g. compare layers 1P and 1H), or the thicknesses of the layers (e.g. veneer versus valley-ponded material in layer 2), showing that these variables did not significantly influence the temperature structure of the deposits. From 30 to 50–60 km from vent, palaeotemperature values ramp upwards, the rise being seen slightly closer to vent in layer 2 than in layer 1 deposits (Fig. 10).

Element c

We find no vertical temperature variation at any site (e.g. Fig. 9b–d).

Implications of temperature data for temporal variations in source temperature

Material deposited closer to source was considerably colder than more-distal deposits (point a, above). The cooler palaeotemperatures in the more-proximal ignimbrite are likely to be primarily due to at least two causes, (1) admixture of a greater bulk content of initially 'cold' lithics, probably amounting to >30 mass% (Wilson 1985), and (2) interaction between the erupted material and remnants of a pre-eruption Lake Taupo which partly surrounded the vent area. Lesser amounts of cooling will also have occurred due to adiabatic decompression (~90 °C in the specific case of this eruption; Mitchell 2001) and mixing with the atmosphere. However, we view large-scale mixing with air as a source of cooling in the current to be unlikely, as high degrees of crystal enrichment, which would be consequently expected as a result of winnowing out of finer, lighter vitric material, are not present in the proximal layer 2 deposits (Wilson 1985).

The part of the current which deposited the hotter, medial to distal parts of the ignimbrite is inferred to have incorporated 16 mass% lithics at source (Wilson 1985), and the juvenile fraction (pumice and ash) to have undergone cooling by ~90 °C by adiabatic decompression (Mitchell 2001). Bulk mixing with the lithics (assumed to be at 20 °C, and to have the same heat capacity as the juvenile material) would reduce the temperature of the overall mixture from the magmatic temperature of 850 °C (Sutton et al. 2000) to about 640 °C. Any further reduction to the T_{eq} estimates of >400 °C could then be accomplished by limited mixing with water or the atmosphere. We know that a considerable number of clasts give emplacement temperatures higher than the equilibrium location mean. We do not yet have a clear understanding of the thermal path experienced by these clasts, so we have used the assumption that the lithic fraction was initially at 20 °C as our working model.

We infer that the main difference in temperature between proximal and distal deposits has arisen from interaction of the proto Lake Taupo with the erupting pyroclastic material which deposited the proximal ignimbrite. It is likely (see also below) that this phreatomagmatic stage occurred during early stages of generation of the Taupo-ignimbrite current, and that the increase in temperature represents the phase when ingress of water to the vent had been reduced (in a similar fashion to the progression of cold-wet to hot-dry ignimbrites erupted from the flooded caldera of the Minoan eruption, on Santorini; Sparks and Wilson 1990). Although the reverse situation is possible, it is less likely on palaeogeographic grounds, since the isopachs of the immediately preceding plinian phase show that the vent was within the confines of the lake, and several of the earlier phases of the 1.8-ka pyroclastic activity (Table 1) display clear evidence of interaction with lake water, suggesting that any pre-1.8 ka dry land within the body of the lake was not extensive.

Implications for emplacement of the Taupo ignimbrite

There are three main elements of the emplacement of the Taupo ignimbrite which need to be addressed, from existing data and our new temperature determinations, in the light of existing models. These are:

1. Was the hotter, medial–distal ignimbrite deposited from material erupted early or late in the short-lived episode which generated the Taupo current? The proximal layer 1 and 2 deposits share similar, low palaeotemperatures (Fig. 10), and so any hotter material which gave rise to the medial–distal ignimbrite did not deposit any material in the proximal area which was detected by our sampling. There are three features which count against the cooler proximal deposits representing later, less-far-travelled stages of the current: (1) the evidence from palaeogeography (above); (2) the evidence for exceptionally high velocities of the current which deposited the proximal ignimbrite (e.g. from the size of megaripple bedforms in the veneer deposits; Wilson 1985); and (3) the absence of any hotter proximal layer 1 deposits deposited from hypothetically earlier stages of the current. We infer that the later, hotter flows must have deposited only a small fraction of the thickness of the ignimbrite in proximal areas, and that these deposits were not represented in our sampling.

2. Did the Taupo ignimbrite deposit evenly throughout its extent, throughout the history of passage of the current, or unevenly? The lack of thermal gradients in the deposits which we sampled (point c, above) suggests that deposition was not even and continuous throughout the extent of the ignimbrite. Previous field-based work had inferred that generation of the current was a short-lived event, such that to a first order, the timescale over which material was ejected to form the current was equal to or shorter than the time taken for the current to propagate from vent to its outer limits (Wilson and Walker 1981). In addition, the layering in the veneer deposit was used to infer that the current was entirely erupted by the time its front had reached to ~40 km from vent, and that the current represented a single, large pulse of material from ~40 km outwards (Wilson and Walker 1981). Thus, we envisage the early, cooler parts of the ignimbrite being erupted and deposited very rapidly, and the current being augmented by hotter material out to the point at which its front had reached ~40 km from vent (cf. temperature variations in Fig. 10). Deposition of material from the current is thus inferred to have progressed from proximal to distal areas, with the changing thermal properties of the current being reflected in changing temperatures recorded in the deposits. The similarity between temperatures in layers 1 and 2, regardless of lithic content (point b, above), implies that the temperatures in the lithics were buffered by, and reflect the bulk temperature of, a much larger mass of material prior to deposition, viz. the moving pyroclastic current.

3. What was the density state of the Taupo current? Two end-member models have been proposed for the Taupo current in particular and other pyroclastic density currents in general. The first model considers the dominant mass of material and momentum to be in a concentrated gas-particle dispersion, with densities and solids concentrations of the order 0.1–1.0 Mg/m^3 and tens of percent respectively (e.g. Sparks 1976; Wilson 1985). A dilute upper suspension cloud is present but is considered to be subordinate to and/or derived from the concentrated dispersion beneath. Deposition of such dispersions can vary between en-masse and layer-by-layer, depending on the velocity of the current and local depositional conditions (Sparks 1976; Wilson 1985; Branney and Kokelaar 1992). The second model treats flows as dilute turbulent suspensions, with densities and solids concentrations of the order 0.001–0.01 Mg/m^3 and <1% respectively (e.g. Bursik and Woods 1996; Dade and Huppert 1996). In this model, the dilute suspension carries most of the mass and momentum of the current, and material is deposited by settling from suspension, or via processing for a short time in a more-concentrated 'depositional system' (Branney and Kokelaar 1992).

Previous studies had suggested that the former model was more appropriate for the Taupo ignimbrite (Wilson 1985, 1997; cf. Dade and Huppert 1996). As the Taupo is an end-member example of energetically emplaced (low-aspect ratio) ignimbrites (Walker 1983), conclusions about the nature of its parental flow have strong implications also for ignimbrite-producing pyroclastic flows in general. However, the flow model involving transport as a dilute turbulent suspension has gained widespread acceptance. Such currents can be readily mathematically modelled using inferences from conventional liquid/liquid gravity currents (e.g. Bursik and Woods 1996; Dade and Huppert 1996; Todesco et al. 2002) and reproduced in laboratory analogue experiments (e.g. Huppert et al. 1986; Woods and Bursik 1994; Choux and Druitt 2002).

The theoretical modelling by Bursik and Woods (1996) divided ignimbrite-producing pyroclastic suspension currents into two categories, one deeper (1–3 km), slower (10–100 m/s) and sub-critical, with little interaction with the atmosphere (and hence limited cooling), the other shallower, faster (100–200 m/s) and supercritical, with significant mixing with the atmosphere (and hence significant cooling effects) and substantially shorter travel distances for a given eruption rate. However, characteristics of the Taupo ignimbrite show such a distinction is contradictory in this case. The Taupo current was emplaced at >150–200 m/s over much of its area of reach (Wilson and Walker 1981; Wilson 1985), i.e. it would have been supercritical by the criteria of Bursik and Woods (1996). However, the distance travelled far exceeds the theoretical limit for a supercritical flow erupted at the appropriate rate (3×10^{10} kg/s; Wilson and Walker 1981; cf. Bursik and Woods 1996, their Fig. 9a). In addition, the temperature data presented here imply that cooling during transport of the Taupo flow (by mixing with air) was of sub-equal or lesser importance than the initial cooling during formation of the current. Thus, in its travel distance and palaeotemperature characteristics, the Taupo more closely follows the sub-critical flow model of Bursik and Woods (1996), but this is contradicted by the demonstrably energetic emplacement of the flow. The palaeotemperature data thus are consistent with the model where a concentrated basal portion of the Taupo flow was present during all but the most-proximal (<13 km) transport, and played a dominant role in emplacement and deposition of the Taupo ignimbrite, despite the high emplacement velocities (Wilson 1985, 1997).

Conclusions

Palaeomagnetic determinations of palaeotemperatures of emplacement from lithic fragments give valuable information about the equilibrium, or 'bulk' temperature of the Taupo ignimbrite, up to a maximum imposed by the highest Curie temperature of the magnetic phases (effectively 580 °C in this case). Apparently plausible temperatures determined from pumices at the same sampling sites are shown to be misleading, as the temperature values obtained are a function of the magnetic mineralogy (itself dependent on the cooling rate), not of the equilibrium temperature of the deposit. The closely coupled values of temperature determined from the various lithic-richer and lithic-poorer facies, and rapidly cooled landscape-mantling deposits versus slower-cooled valley-ponded deposits are consistent with all the ignimbrite facies (and their associated temperature determinations) being derived from a single flow. Earlier-erupted portions of this flow were cooler (~200 °C) whereas later-erupted portions, which travelled farther from source, were hotter (>400 °C). The greater cooling of the earlier material is primarily attributed to mixing with lake water and incorporation of the lithic fragments themselves (most, but not all, of which were apparently 'cold' on incorporation). Mixing with air during eruption is inferred to be of secondary importance. The inferred temperature structure of the ignimbrite supports the notion that the parental current was a relatively concentrated system for most of its travel distance.

References

Aramaki S, Akimoto S (1957) Temperature estimation of pyroclastic deposits by natural remanent magnetism. Am J Sci 255:619–627

Bahar D, Smith GA, Geissman JW, Grubensky MJ (1993) Estimated paleomagnetic emplacement temperatures of the Taupo

ignimbrite, New Zealand: defining thermal characteristics of a pyroclastic flow (abstract). EOS Trans AGU 74(Suppl 43):639

Bardot L (2000) Emplacement temperature determinations of proximal pyroclastic deposits on Santorini, Greece, and their implications. Bull Volcanol 61:450–467

Bardot L, McClelland E (2000) The reliability of emplacement temperature estimates using paleomagnetic methods: a case study from Santorini, Greece. Geophys J Int 143:39–51

Bardot L, Thomas R, McClelland E (1996) Emplacement temperatures of pyroclastic deposits on Santorini deduced from paleomagnetic measurements: constraints on eruption mechanisms. In: Morris A, Tarling DH (eds) Paleomagnetism and tectonics of the Mediterranean region. Geol Soc Lond Spec Publ 105:345–358

Bierwirth PN (1982) Experimental welding of volcanic ash. BSc (Hons) Thesis, Monash University, Clayton, Victoria, Australia

Branney MJ, Kokelaar BP (1992) A reappraisal of ignimbrite emplacement: progressive aggradation and changes from particulate to non-particulate flow during emplacement of high-grade ignimbrite. Bull Volcanol 54:504–520

Bursik MI, Woods AW (1996) The dynamics and thermodynamics of large ash flows. Bull Volcanol 58:175–193

Cas RAF, Wright JV (1987) Volcanic successions modern and ancient. Allen & Unwin, London, pp 1–528

Chernet T (1987) Lithic inclusions in the Taupo Pumice Formation. MSc Thesis, Victoria University, Wellington, New Zealand

Choux CM, Druitt TH (2002) Analogue study of particle segregation in pyroclastic density currents, with implications for the emplacement mechanisms of large ignimbrites. Sedimentology 49:907–928

Cole JW, Brown SJA, Burt RM, Beresford SW, Wilson CJN (1998) Lithic types in ignimbrites as a guide to the evolution of a caldera complex: Taupo volcanic centre, New Zealand. J Volcanol Geotherm Res 80:217–237

Dade WB, Huppert HE (1996) Emplacement of the Taupo ignimbrite by a dilute turbulent flow. Nature 381:509–512

Dade WB, Huppert HE (1997) Emplacement of the Taupo ignimbrite (reply to comments by CJN Wilson). Nature 385:306–307

Dodson MH, McClelland-Brown E (1980) Magnetic blocking temperatures during slow cooling. J Geophys Res 85:2625–2637

Donoghue SL, Palmer AS, McClelland E, Hobson K, Stewart RB, Neall VE, Lecointre J, Price R (1999) The Taurewa eruptive episode: evidence for climactic eruptions at Ruapehu volcano, New Zealand. Bull Volcanol 60:223–240

Downey WS, Tarling DH (1984) Archaeomagnetic dating of Santorini volcanic eruptions and fired destruction levels of late Minoan civization. Nature 309:519–523

Friedman I, Long W, Smith RL (1963) Viscosity and water contents of rhyolitic glass. J Geophys Res 68:6523–6535

Henry CD, Wolff JA (1992) Distinguishing strongly rheomorphic tuffs from extensive silicic lavas. Bull Volcanol 54:171–186

Hoblitt RP, Kellogg KS (1979) Emplacement temperatures of unsorted and unstratified deposits of volcanic rock debris as determined by paleomagnetic techniques. Geol Soc Am Bull Part I 90:633–642

Huppert HE, Turner JS, Carey SN, Sparks RSJ, Hallworth MA (1986) A laboratory study of pyroclastic flows down slopes. J Volcanol Geotherm Res 30:179–199

Jaeger JC (1964) Thermal effects of intrusions. Rev Geophys 2:443–466

Kent DV, Ninkovitch D, Pescatore T, Sparks RSJ (1981) Paleomagnetic determination of emplacement temperature of the Vesuvius AD 79 pyroclastic deposits. Nature 290:393–396

Kent JT, Briden JC, Mardia KV (1983) Linear and planar structure in ordered multivariate data as applied to progressive demagnetization of paleomagnetic remanence. Geophys J R Astron Soc 75:593–621

Kono Y, Osima Y (1971) Numerical experiments on the welding processes in the pyroclastic flow deposits. Bull Volcanol Soc Japan 16:1–14

Lindsley DH (ed) (1991) Oxide minerals: petrologic and magnetic significance. Mineral Soc Am Rev Mineral 25:1–509

Mandeville CW, Carey S, Sigurdsson H, King J (1994) Paleomagnetic evidence for high-temperature emplacement of the 1883 subaqueous pyroclastic flows from Krakatau volcano, Indonesia. J Geophys Res 99:9487–9504

Maury R (1971) Application de la spectrométrie infrarouge à l'étude des bois fossilisés dans les formations volcaniques. Bull Soc Géol Fr (7)XIII:532–538

McClelland E (1996) Theory of CRM acquired by grain growth, and its implications for TRM discrimination and paleointensity determination in igneous rocks. Geophys J Int 126:271–280

McClelland E, Druitt TH (1989) Paleomagnetic estimation of emplacement temperatures of pyroclastic deposits on Santorini, Greece. Bull Volcanol 51:16–27

McClelland E, Thomas RME (1990) A paleomagnetic study of Minoan age tephra from Thera. In: Hardy DA, Keller J, Galanopoulos VP, Flemming NC, Druitt TH (eds) Thera and the Aegean World III, vol 2 (Earth Sciences). The Thera Foundation, London, pp 129–139

McClelland-Brown E (1982) Discrimination of TRM and CRM by blocking temperature spectrum analysis. Phys Earth Planet Inter 30:405–414

Mitchell KL (2001) The thermodynamics and fluid mechanics of explosive volcanic eruptions on the Earth and Mars. PhD Thesis, Lancaster University

Riehle JR (1973) Calculated compaction profiles of rhyolitic ash-flow tuffs. Geol Soc Am Bull 84:2193–2216

Riehle JR, Miller TF, Bailey RA (1995) Cooling, degassing and compaction of rhyolitic ash flow tuffs: a computational model. Bull Volcanol 57:319–336

Smith RT, Houghton BF (1995) Vent migration and changing eruptive style during the 1800 a Taupo eruption: evidence from the Hatepe and Rotongaio phreatoplinian ashes. Bull Volcanol 57:432–439

Sparks RSJ (1976) Grain size variations in ignimbrites and implications for the transport of pyroclastic flows. Sedimentology 23:147–188

Sparks RSJ, Wilson CJN (1990) The Minoan deposits: a review of their characteristics and interpretation. In: Hardy DA, Keller J, Galanopoulos VP, Flemming NC, Druitt TH (eds) Thera and the Aegean World III, Volume 2 (Earth Sciences). The Thera Foundation, London, pp 89–99

Sparks RSJ, Self S, Walker GPL (1973) Products of ignimbrite eruptions. Geology 1:115–118

Sutton AN, Blake S, Wilson CJN (1995) An outline geochemistry of rhyolite eruptives from Taupo volcanic centre, New Zealand. J Volcanol Geotherm Res 68:153–175

Sutton AN, Blake S, Wilson CJN, Charlier BLA (2000) Late Quaternary evolution of a hyperactive rhyolite magmatic system: Taupo volcanic centre, New Zealand. J Geol Soc Lond 157:537–552

Todesco M, Neri A, Esposito Ongaro T, Papale P, Macedonio G, Santacroce R, Longo, A (2002) Pyroclastic flow hazard assessment at Vesuvius (Italy) by using numerical modeling. I. Large-scale dynamics. Bull Volcanol 64:155–177

Tsuboi S, Tsuya H (1930) On the temperature of the pumiceous ejecta of Komagatake, Hokkaidò, as inferred from their modes of oxidation. Bull Earthq Res Inst Univ Tokyo 8:271–273

Walker GPL (1983) Ignimbrite types and ignimbrite problems. J Volcanol Geotherm Res 17:65–88

Walker GPL, Heming RF, Wilson CJN (1980) Low-aspect ratio ignimbrites. Nature 283:286–287

Walker GPL, Self S, Froggatt PC (1981a) The ground layer of the Taupo ignimbrite: a striking example of sedimentation from a pyroclastic flow. J Volcanol Geotherm Res 10:1–11

Walker GPL, Wilson CJN, Froggatt PC (1981b) An ignimbrite veneer deposit: the trail marker of a pyroclastic flow. J Volcanol Geotherm Res 9:409–421

Watson GS (1956) A test for randomness. Mon Notes R Astron Soc 7:160–161

Wilson CJN (1985) The Taupo eruption, New Zealand. II. The Taupo ignimbrite. Philos Trans R Soc Lond A314:229–310

Wilson CJN (1993) Stratigraphy, chronology, styles and dynamics of late Quaternary eruptions from Taupo volcano, New Zealand. Philos Trans R Soc Lond A343:205–306

Wilson CJN (1997) Emplacement of the Taupo ignimbrite. Nature 385:306–307

Wilson CJN, Hildreth W (2003) Assembling an ignimbrite: mechanical and thermal building blocks in the Bishop Tuff, California. J Geol 111:653–670

Wilson CJN, Walker GPL (1981) Violence in pyroclastic flow eruptions. In: Self S, Sparks RSJ (eds) Tephra studies. D. Reidel, Dordrecht, The Netherlands, pp 441–448

Wilson CJN, Walker GPL (1982) Ignimbrite depositional facies: the anatomy of a pyroclastic flow. J Geol Soc Lond 139:581–592

Wilson CJN, Walker GPL (1985) The Taupo eruption, New Zealand. I. General aspects. Philos Trans R Soc Lond A314:199–228

Woods AW, Bursik MI (1994) A laboratory study of ash flows. J Geophys Res 99:4375–4393

Yagi K (1966) Experimental study on pumice and obsidian. Bull Volcanol 29:559–572

Zlotniki J, Pozzi JP, Boudon G, Moreau MG (1984) A new method for the determination of the setting temperature of pyroclastic deposits (example of Guadeloupe: French West Indies). J Volcanol Geotherm Res 21:297–312